

FLUCTUATIONS OF SCHENSTED ROW INSERTION

MIKOŁAJ MARCINIAK AND PIOTR ŚNIADY

ABSTRACT. We investigate several asymptotic probabilistic questions related to random Young tableaux and *the Schensted row insertion* which is the key component of the Robinson–Schensted–Knuth algorithm (RSK). For example, for a random tableau T with a specified shape λ we investigate the relationship between (i) the position of the new box created in the row insertion $T \leftarrow z$ when a new entry z is inserted into the tableau T , and, (ii) the value of the new entry z being inserted. Since the tableau T is random, the aforementioned relationship is random as well; we investigate its fluctuations around the mean value, in the limit as the number of boxes of the Young diagram λ tends to infinity. Our results can be also used to prove the asymptotic Gaussianity of the last entry of the first row in a uniformly random standard Young tableau with some prescribed large shape.

1. TEASER: NEW CONJECTURES RELATED TO RSK ALGORITHM APPLIED TO RANDOM INPUT

This paper is quite long; in order to motivate the reader we start with a teaser: two new conjectures (Conjecture 1.5 and Conjecture 1.7) which concern RSK algorithm applied to a random input.

1.1. Basic definitions. We start by recalling some basic combinatorial notions. For a more detailed treatment of the topic, we refer to [Ful97].

1.1.1. Young diagrams, tableaux. A Young diagram is a finite collection of boxes on the positive quarterplane, aligned to the left and to the bottom, see Figure 1a. This way of drawing Young diagrams is called *the French convention*. To a Young diagram with ℓ rows we associate the integer partition $\lambda = (\lambda_1, \dots, \lambda_\ell)$, where λ_j denotes the number of the boxes in the j -th row (we count the rows from bottom to top). We identify a Young diagram with the corresponding partition λ and denote by $|\lambda| = \lambda_1 + \dots + \lambda_\ell$ the number of its boxes.

2020 *Mathematics Subject Classification.* 60C05 (Primary); 60F05, 05E10, 20C30, 60K35, 82C22 (Secondary).

Key words and phrases. Robinson–Schensted correspondence, Schensted row insertion, random Young tableaux, limit shape, jeu de taquin, second class particles.

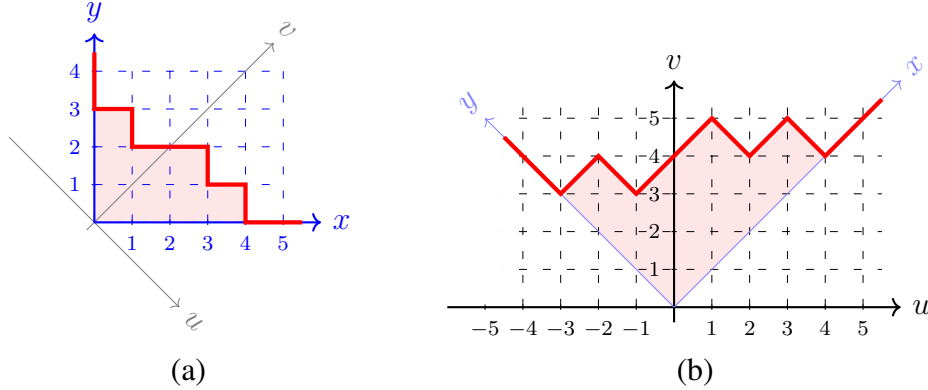


Figure 1. The Young diagram $(4, 3, 1)$ shown in (a) the French convention, and (b) the Russian convention. The solid red line represents the *profile* of the Young diagram. The coordinates system (u, v) corresponding to the Russian convention and the coordinate system (x, y) corresponding to the French convention are shown.

A *tableau* is a filling of the boxes of a Young diagram with numbers; we require that the entries should be weakly increasing in each row (from left to right) and strictly increasing in each column (from bottom to top). An example is given in Figure 2a. We say that a tableau T of shape λ is a *standard Young tableau* if it contains only entries from the set $\{1, 2, \dots, |\lambda|\}$ and each element is used exactly once.

1.1.2. Schensted insertion. The *Schensted row insertion* is an algorithm which takes as an input a tableau T and some number z . The number z is inserted into the first row (i.e., the bottom row) of T in the leftmost box which contains an entry which is strictly bigger than z .

In the case when the row contains no entries which are bigger than z , the number z is inserted into the leftmost empty box in this row and the algorithm terminates.

If, however, the number z was inserted into a box which was not empty, the previous content z' of the box is *bumped* into the second row. This means that the algorithm is iterated but this time the number z' is inserted into the second row in the leftmost box which contains a number bigger than z' ; if necessary this is repeated until some number is inserted into a previously empty box. This process is illustrated in Figures 2b and 2c. The outcome of Schensted insertion is defined as the new resulting tableau; it will be denoted by $T \leftarrow z$.

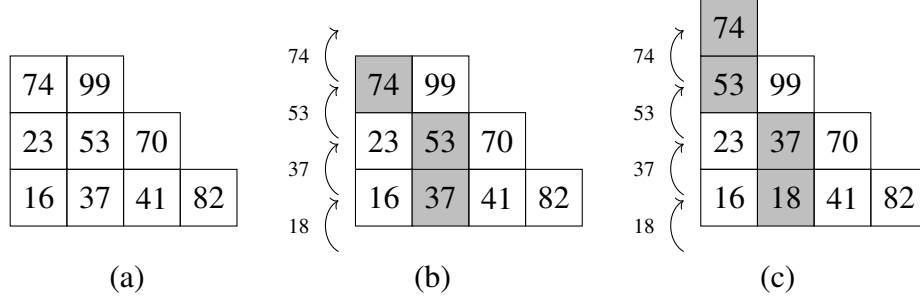


Figure 2. (a) The original tableau T . (b) The highlighted boxes form the bumping route which corresponds to a Schensted insertion $T \leftarrow 18$. The numbers next to the arrows indicate the bumping entries. (c) The output $T \leftarrow 18$ of the Schensted insertion.

The *bumping route* consists of the boxes whose content has changed by the action of Schensted insertion, see Figures 2b and 2c.

1.1.3. Robinson–Schensted–Knuth algorithm. For the purposes of this article we consider a simplified version of *Robinson–Schensted–Knuth algorithm*; for this reason we should rather call it *Robinson–Schensted algorithm*. Nevertheless, we use the first name because of its well-known acronym RSK. The RSK algorithm associates to a finite sequence $w = (w_1, \dots, w_n)$ a pair of tableaux: the *insertion tableau* $P(w)$ and the *recording tableau* $Q(w)$.

The insertion tableau

$$(1.1) \quad P(w) = \left(((\emptyset \leftarrow w_1) \leftarrow w_2) \leftarrow \dots) \leftarrow w_n \right)$$

is defined as the result of iterative Schensted insertion applied to the entries of w , starting from the empty tableau \emptyset .

The recording tableau $Q(w)$ is defined as the standard Young tableau of the same shape as $P(w)$ in which each entry is equal to the number of the iteration of (1.1) in which the given box stopped being empty; in other words the entries of $Q(w)$ give the order in which the entries of the insertion tableau were filled.

Tableaux $P(w)$ and $Q(w)$ have the same shape; we will denote this common shape by $\text{RSK}(w)$ and call it *the RSK shape associated to w* .

The RSK algorithm is an important tool of algebraic combinatorics and representation theory, especially in the context of the Littlewood–Richardson coefficients, see [Ful97; Sta99].

1.2. Context and motivations. A fruitful area of research is to investigate the RSK algorithm applied to a random input. We shall review below some selected highlights of this area.

1.2.1. Plancherel measure. The simplest example concerns the case when $w = (w_1, \dots, w_n)$ is a uniformly random permutation in n letters. Since the recording tableau depends only on the relative order of the entries which form the input, the probability distribution of the recording tableau $Q(w)$ would not change if we replace the above probability distribution and take $w = (w_1, \dots, w_n)$ to be a sequence of independent, identically distributed random variables with the uniform distribution $U(0, 1)$ on the unit interval $[0, 1]$. The corresponding probability distribution of $\text{RSK}(w)$ is the celebrated *Plancherel measure* Pl_n on the set of Young diagrams with n boxes which appears naturally in the context of decomposition of the left regular representation of the symmetric group \mathfrak{S}_n into irreducible components. This measure associates to a Young diagram λ (such that $|\lambda| = n$) the probability

$$\text{Pl}_n(\lambda) = \frac{(f^\lambda)^2}{n!},$$

where f^λ denotes the number of standard Young tableaux of shape λ .

The most spectacular highlight related to the probability distribution of $\text{RSK}(w)$ is the solution of the *Ulam–Hammersley problem* [BDJ99; Oko00] which shows a surprising link with the *Tracy–Widom distribution* which arises in random matrix theory. For a pedagogical introduction to this topic we recommend the book [Rom15].

1.2.2. Extremal characters of \mathfrak{S}_∞ . If w_1, w_2, \dots is a sequence of independent, identically distributed random variables (possibly with a more complicated probability distribution which might have some atoms), and

$$(1.2) \quad \lambda^{(n)} = \text{RSK}(w_1, \dots, w_n)$$

denotes the RSK shape corresponding to a prefix of size n , we may regard the growing sequence of Young diagrams

$$(1.3) \quad \emptyset = \lambda^{(0)} \nearrow \lambda^{(1)} \nearrow \dots$$

as a Markov random walk in the *Young graph* which is a directed graph having the Young diagrams as the vertices and directed edges connecting pairs of diagrams which differ by exactly one box. This random walk (1.3) has some additional convenient properties which are out of scope of the current paper. Vershik and Kerov [VK81; KV86] proved that a classification of the random walks with such additional properties (which is a problem on the boundary between probability theory, harmonic analysis on the Young graph, and ergodic theory) is equivalent to finding the *extremal characters*

of the infinite symmetric group \mathfrak{S}_∞ . In this way Vershik and Kerov found a new, truly conceptual proof of Thoma's classification of such characters [Tho64]. As a byproduct, there is a convenient bijection between the extremal characters of \mathfrak{S}_∞ and the probability laws of the random variables (w_n) , and RSK provides a convenient, explicit way of generating the corresponding random walk (1.3).

1.2.3. *The key motivation: is RSK an isomorphism of dynamical systems?*
The recording tableau

$$Q_\infty(w_1, w_2, \dots) := \lim_{n \rightarrow \infty} Q(w_1, \dots, w_n)$$

corresponding to an *infinite* sequence w_1, w_2, \dots is an *infinite standard tableau*, i.e., a filling of the boxes in (a subset of) the upper-right quarterplane such that each natural number appears exactly once. Just like its finite counterpart from Section 1.1.3, each entry of the infinite recording tableau $Q_\infty(w_1, w_2, \dots)$ is equal to the number of the iteration of an infinite sequence of row insertions

$$((\emptyset \leftarrow w_1) \leftarrow w_2) \leftarrow \dots$$

in which the given box stopped being empty. This infinite recording tableau is another way of encoding the infinite path (1.3) in the Young graph.

The aforementioned link between RSK and the Plancherel measure can be rephrased in a more abstract way as follows: Q_∞ is a homomorphism between the following two probability spaces:

- the infinite Cartesian power $[0, 1]^\infty$ of the unit interval, equipped with the product of the Lebesgue measure (which clearly corresponds to a sequence w_1, w_2, \dots of independent, identically distributed random variables with the uniform distribution on the unit interval),

and

- the set of infinite standard Young tableaux equipped with the *Plancherel measure* (which in light of the aforementioned results of Vershik and Kerov is fundamental for harmonic analysis on the infinite symmetric group \mathfrak{S}_∞).

In fact, each of these two probability spaces can be equipped with a natural measure-preserving transformation (respectively, the *one-sided shift* and the *jeu de taquin transformation*) in such a way that Q_∞ becomes a homomorphism between two *measure-preserving dynamical systems*. It is natural to ask the following question.

Problem 1.1 (The key motivation). *Is it true that Q_∞ is, in fact, an isomorphism of dynamical systems? If yes, how to construct the inverse map?*

The answer is not immediately obvious because in the finite case, when RSK is applied to a *finite* sequence w , in order to recover w we need information about the recording tableau $Q(w)$, *as well as about the insertion tableau* $P(w)$; the latter is *not* available in the infinite case. An affirmative answer to Problem 1.1 would shed light on some questions related to the harmonic analysis on \mathfrak{S}_∞ , for example whether jeu de taquin is ergodic.

These motivations were the starting point for the work of Romik and the second named author [RS15]; we present their findings in the following. Spoiler alert: Problem 1.1 has an affirmative answer.

1.3. The main problem: position of the new box. For asymptotic problems it is convenient to draw the Young diagrams in the *Russian convention*, see Figure 1b, which corresponds to the coordinate system (u, v) which is related to the usual (French) Cartesian coordinates by

$$u = x - y, \quad v = x + y.$$

For a finite sequence $w = (w_1, \dots, w_{n+1})$ we denote by

$$\text{Ins}(w_1, \dots, w_n; w_{n+1}) = (x_n, y_n)$$

the coordinates of the last box which was inserted to the Young diagram by the RSK algorithm applied to the sequence w . In other words, it is the box containing the biggest number in the recording tableau $Q(w)$. Above, (x_n, y_n) refer to the Cartesian coordinates of this box in the French convention, i.e., x_n is the number of the column and y_n is the number of the row. By

$$u\text{-Ins}(w_1, \dots, w_n; w_{n+1}) = x_n - y_n$$

we denote the u -coordinate of the aforementioned box.

For later use, given a tableau T and a real number z we denote by $\text{Ins}(T; z)$ the coordinates of the new box which was created by the Schensted row insertion $T \leftarrow z$; in other words it is the unique box of the skew diagram

$$\text{shape}(T \leftarrow z) \setminus \text{shape } T;$$

the quantity $u\text{-Ins}(T; z)$ is defined in an analogous way as the u -coordinate of $\text{Ins}(T; z)$.

In the current paper we concentrate on the aforementioned fundamental case when w_1, w_2, \dots is a sequence of independent, identically distributed random variables with the uniform distribution $U(0, 1)$ on the unit interval $[0, 1]$. Romik and the second named author [RS15] noticed that the construction of the inverse map to Q_∞ (and, in consequence, a positive answer to Problem 1.1) requires a solution to the following somewhat vague question about the usual (finite) version of RSK applied to such a random input.

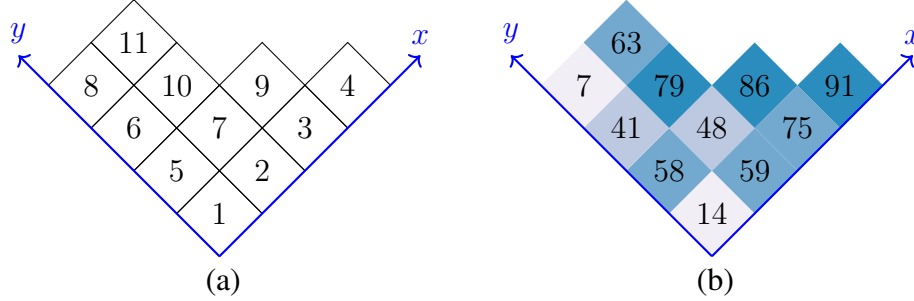


Figure 3. (a) The recording tableau $Q_{xy} = Q(w)$ (drawn in the Russian convention) which corresponds to the sequence $w = (14, 59, 75, 91, 58, 41, 48, 7, 86, 79, 63)$ which was selected from the interval $J = [0, 100]$. (b) The responsibility matrix $(w_{Q_{xy}})$ obtained by replacing each entry of the recording tableau by the corresponding entry of the sequence w . The following layer tinting was used: the four colors of the background correspond to the values of the responsibility matrix in the four quarters of the interval J , namely, $[0, 25]$ (almost white), $(25, 50]$ (beige), $(50, 75]$ (blue), and $(75, 100]$ (dark blue).

Problem 1.2 (The main problem). *Let $w = (w_1, w_2, \dots)$ be a sequence of independent, identically distributed random variables with the uniform distribution $U(0, 1)$ on the unit interval.*

What is the relationship between

- *the value of the new entry w_{n+1} , and*
- *the position of the corresponding newly created box*

$$(1.4) \quad (x_n, y_n) = \text{Ins}(w_1, \dots, w_n; w_{n+1})?$$

We are interested in this probabilistic question in the limit as $n \rightarrow \infty$.

This problem can be visualized by replacing the number in any box $\square = (x, y)$ of the recording tableau $(Q_{xy}) = Q(w)$ by the entry of the sequence $w = (w_1, \dots, w_n)$ which was responsible for the creation of \square . The resulting matrix $(w_{Q_{xy}})$ will be called *the responsibility matrix*, see Figure 3b for an example. In order to improve legibility and avoid writing real numbers, the entries of the sequence w in the example in Figure 3 are integers sampled from the interval $J = [0, 100]$.

Following the ideas of Pittel and Romik [PR07, Section 1.1], the responsibility matrix can be depicted geometrically as a three-dimensional stack of cuboids over the plane $\mathbb{R}^2 \times \{0\}$, where $w_{Q_{xy}}$ is the height of the cuboid

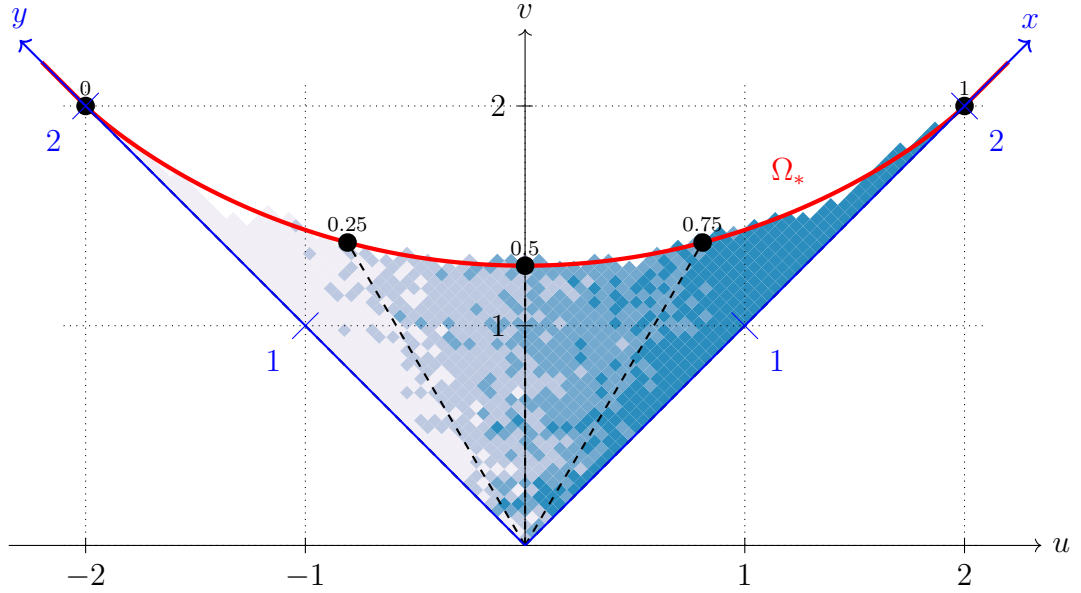


Figure 4. An analogue of Figure 3b for a sequence $w = (w_1, \dots, w_{1000})$ of $n = 1000$ independent, identically distributed random variables with the uniform distribution $U(0, 1)$ on the unit interval $I = [0, 1]$. The layer tinting indicates the values of the responsibility matrix $(w_{Q_{xy}})$: the four colors correspond to the values in the four intervals $[0, 1/4]$ (almost white), $(1/4, 1/2]$, $(1/2, 3/4]$, $(3/4, 1]$ (dark blue). The red solid line is the Logan–Shepp–Vershik–Kerov limit curve Ω_* . The five black dots indicate its natural parametrization; they divide the area between the curve and the Oxy axes into four curvilinear triangles of equal areas.

which has the unit square $[x - 1, x] \times [y - 1, y] \times \{0\}$ as the base. Alternatively, the function $(x, y) \mapsto w_{Q_{xy}}$ can be thought of as the graph of the (non-continuous) surface of the upper envelope of this stack. By rescaling the unit squares on the plane $\mathbb{R}^2 \times \{0\}$ to be squares of side length $\frac{1}{\sqrt{n}}$ (recall that n is the length of the sequence w), the total base area of the cuboids becomes equal to 1, see Figure 4 for an example. In Figures 3b and 4 the elevation (i.e., the values of the responsibility matrix) was indicated by *layer tinting*.

Monte Carlo simulations such as the one from Figure 4 suggest that the value of the new entry w_{n+1} in Problem 1.2 determines the ray (a halfline starting in the origin of the coordinate system) on which the coordinates $\text{Ins}(w_1, \dots, w_n; w_{n+1})$ will approximately appear (with high probability,

asymptotically, as $n \rightarrow \infty$). Small values of the new entry (i.e., $w_{n+1} \approx 0$) seem to correspond to the rays closer to the Oy axis (the almost white area in Figure 4) while large values ($w_{n+1} \approx 1$) seem to correspond to the rays closer to the Ox axis (the dark blue area in Figure 4).

1.4. The limit shape and its parametrization. The first step towards understanding Problem 1.2 is the simple observation that the newly created box $\text{Ins}(w_1, \dots, w_n; w_{n+1})$ must be located in one of the concave corners of the Young diagram $\lambda^{(n)} = \text{RSK}(w_1, \dots, w_n)$. For this reason, for our purposes it is beneficial to understand the asymptotic behavior of the random Young diagram $\lambda^{(n)}$. Fortunately, the probability distribution of such a RSK shape is simply the Plancherel measure on Young diagrams with n boxes for which the limit shape is well-known; we will review it in the following. For a pedagogical introduction to this topic we refer to [Rom15, Chapter 1].

1.4.1. Scaling of Young diagrams. The boundary of a Young diagram λ is called its *profile*, see Figure 1a. In the Russian coordinate system the profile can be seen as the plot of the function $\omega_\lambda: \mathbb{R} \rightarrow \mathbb{R}_+$, see Figure 1b.

If $c > 0$ is a positive number, the output $c\lambda \subset \mathbb{R}_+^2$ of a homogeneous dilation with scale c applied to the Young diagram λ might no longer be a Young diagram. Nevertheless, its profile is still well defined as

$$\omega_{c\lambda}(u) = c \omega_\lambda\left(\frac{u}{c}\right).$$

1.4.2. The Logan–Shepp–Vershik–Kerov limit shape. Independently Logan and Shepp [LS77] as well as Vershik and Kerov [VK77] proved that a law of large numbers for the shapes holds true: as the number of boxes $n \rightarrow \infty$ tends to infinity, the scaled down profile of the random Young diagram converges in probability to some explicit limit curve, see Figure 4 for an illustration.

Define the function $\Omega_*: \mathbb{R} \rightarrow [0, \infty)$ by

$$(1.5) \quad \Omega_*(u) = \begin{cases} \frac{2}{\pi} \left[u \sin^{-1}\left(\frac{u}{2}\right) + \sqrt{4 - u^2} \right] & \text{if } -2 \leq u \leq 2, \\ |u| & \text{otherwise.} \end{cases}$$

Theorem 1.3 (The limit shape of Plancherel-distributed Young diagrams [LS77; VK77]). *Let $\lambda^{(n)}$ be a random Young diagram distributed according to the Plancherel measure on Young diagrams with n boxes. Then we have a convergence in the supremum norm in probability*

$$\sup_{u \in \mathbb{R}} \left| \omega_{\frac{1}{\sqrt{n}}\lambda^{(n)}}(u) - \Omega_*(u) \right| \xrightarrow[n \rightarrow \infty]{P} 0.$$

In fact, the rate of convergence is quite fast and there are some quite precise results about the magnitude of the local fluctuations [BS07].

1.4.3. Location of a box with a specified entry. In the context of Problem 1.2, suppose for a moment that we *do not* know the value of the new entry w_{n+1} . Then the complete answer to Problem 1.2 would be the probability distribution of the new box (1.4). This probability distribution coincides with the distribution of the box containing the entry $n + 1$ in a large Plancherel-distributed random standard Young tableau. An analogous problem was studied by Pittel and Romik [PR07, Section 1.2] for a different class of random tableaux.

Not very surprisingly, the probability distribution of this vector (after rescaling, and in the Russian coordinates)

$$(u_n, v_n) = \left(\frac{x_n - y_n}{\sqrt{n}}, \frac{x_n + y_n}{\sqrt{n}} \right)$$

converges, as $n \rightarrow \infty$, to a certain probability measure μ_* which is supported on the limit curve Ω_* . In order to specify this measure uniquely it is enough to find the limit distribution for the u -coordinates, i.e., for the random variables (u_n) . It turns out that the sequence (u_n) converges in distribution to the *semicircle measure* on the interval $[-2, 2]$, see [Ker93] and [RS15, Theorem 3.2]. The density of this measure is given by

$$f_{\text{SC}}(u) = \frac{1}{2\pi} \sqrt{4 - u^2} \quad \text{for } u \in [-2, 2].$$

We denote by $F_{\text{SC}}: [-2, 2] \rightarrow [0, 1]$ the cumulative distribution function of this semicircle law, given by

$$F_{\text{SC}}(u) = \frac{1}{2\pi} \int_{-2}^u \sqrt{4 - z^2} \, dz \quad \text{for } u \in [-2, 2].$$

1.4.4. The natural parametrization of the limit curve. The following two *RSK-trigonometric functions*

$$\begin{aligned} \text{RSKcos } z &= F_{\text{SC}}^{-1}(z), \\ \text{RSKsin } z &= \Omega_*(F_{\text{SC}}^{-1}(z)) \end{aligned}$$

are defined for $z \in [0, 1]$. The map

$$(1.6) \quad [0, 1] \ni z \mapsto (\text{RSKcos } z, \text{RSKsin } z) \in \mathbb{R}^2$$

is a two-dimensional analogue of the *quantile function* (the inverse of the cumulative distribution function) in the context of the limit measure μ_* . This map provides a convenient parametrization of the limit curve Ω_* , see

the five black dots in Figure 4. It is a natural analogue of the parametrization of the unit circle by the angle

$$z \mapsto (\cos z, \sin z)$$

as well as the parametrization of the hyperbole by the hyperbolic angle

$$z \mapsto (\cosh z, \sinh z)$$

since in all three cases the area of the curvilinear triangle between the the ray, the curve, and the y -axis (respectively, x -axis) is proportional to the value of the parameter z .

1.5. The first main conjecture: the fluctuations of Schensted row insertion. The most convenient way to state an answer to Problem 1.2 is by conditioning, i.e., assuming that the random variable w_{n+1} takes some fixed value $z \in [0, 1]$. The following result of Romik and the second named author provides a first order asymptotics.

Theorem 1.4 ([RS15, Theorem 5.1]). *Let $z \in [0, 1]$ be fixed; we denote by*

$$(u_0, v_0) = (\text{RSKcos } z, \text{RSKsin } z)$$

the corresponding point on the limit curve Ω_ via (1.6).*

Let w_1, w_2, \dots be a sequence of independent, identically distributed random variables with the uniform distribution $U(0, 1)$ on the unit interval; we denote

$$(x_n, y_n) = \text{Ins}(w_1, \dots, w_n; z).$$

Then we have the following convergence in probability:

$$(1.7) \quad \left(\frac{x_n - y_n}{\sqrt{n}}, \frac{x_n + y_n}{\sqrt{n}} \right) \xrightarrow[n \rightarrow \infty]{P} (u_0, v_0).$$

This relationship between the value of the new entry being inserted and the location of the corresponding new box was visualized in Figure 4 by the layer tinting. Theorem 1.4 was illustrated by a Monte Carlo simulation in Figure 5.

We conjecture that the ultimate answer to Problem 1.2 is as follows.

Conjecture 1.5 (The first main conjecture). *We keep the notation from Theorem 1.4.*

Then the scaled sequence of random points

$$(1.8) \quad \sqrt[4]{n} \left[\left(\frac{x_n - y_n}{\sqrt{n}}, \frac{x_n + y_n}{\sqrt{n}} \right) - (u_0, v_0) \right] = \left(\frac{x_n - y_n}{\sqrt[4]{n}} - \sqrt[4]{n} u_0, \frac{x_n + y_n}{\sqrt[4]{n}} - \sqrt[4]{n} v_0 \right) \in \mathbb{R}^2$$

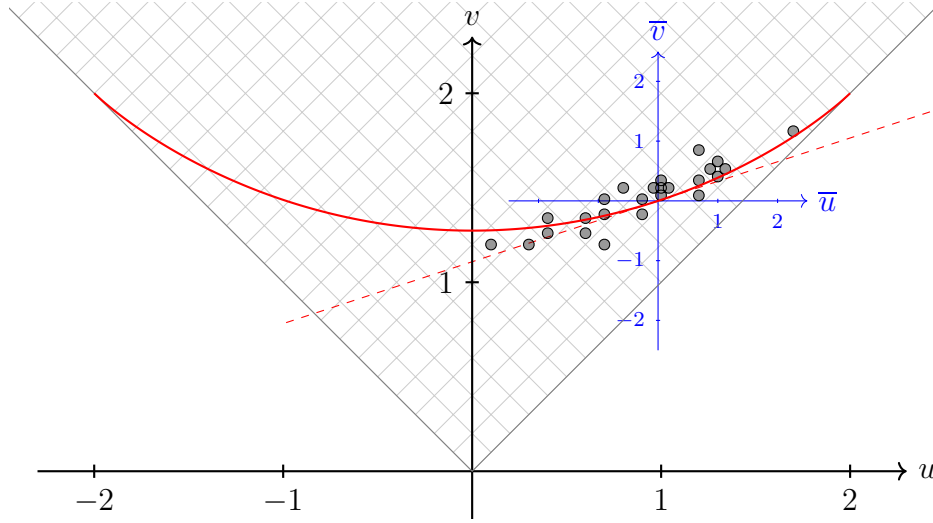


Figure 5. Grey circles indicate simulated (rescaled) positions of the new box $\text{Ins}(w_1, \dots, w_n; z)$ for the initial sequence w_1, \dots, w_n of i.i.d. $U(0, 1)$ random variables of length $n = 100$ and the new entry $z = 0.8$. The uv coordinates of the circles are the quantities which appear in the law of large numbers (Theorem 1.4). The grid indicates the actual size of the boxes. The solid red curve is the Logan–Shepp–Vershik–Kerov limit shape; the red dashed line is tangent to this curve at the point which in the natural parametrization corresponds to z . The coordinates of the circles in the blue (\bar{u}, \bar{v}) coordinate system correspond to the quantities in Conjecture 1.5.

converges in distribution to a centered, degenerate Gaussian distribution on the plane which is supported on the line

$$(1.9) \quad \{(u, v) : v = \Omega'_*(u_0) u\}$$

which is parallel to the tangent line to the limit curve Ω_* in u_0 .

This Gaussian distribution is uniquely determined by the limit measure for the u -coordinates, which is as follows:

$$\sqrt[4]{n} \left[\frac{x_n - y_n}{\sqrt{n}} - u_0 \right] \xrightarrow[n \rightarrow \infty]{d} N(0, \sigma_{u_0}^2).$$

It converges, as $n \rightarrow \infty$, in distribution to the centered normal distribution with the variance

$$(1.10) \quad \sigma_{u_0}^2 = \frac{\pi}{3} \sqrt{4 - u_0^2}.$$

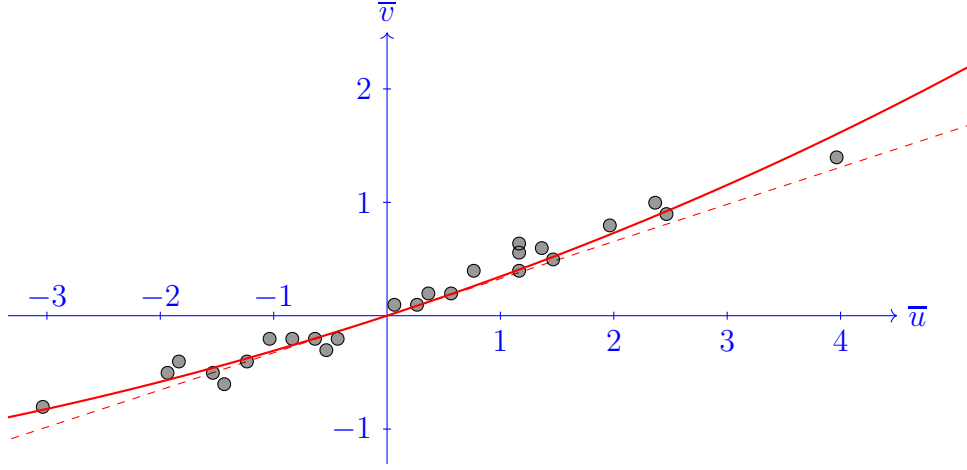


Figure 6. An analogue of Figure 5 for the length of the sequence $n = 10^4$ and $z = 0.8$. The picture was zoomed to focus on the (\bar{u}, \bar{v}) coordinate system. In order to improve visibility the grid with the actual size of the boxes was not shown.

This conjecture is visualized by Monte Carlo simulations in Figures 5 and 6. The blue coordinate system (\bar{u}, \bar{v})

$$(\bar{u}, \bar{v}) = \sqrt[4]{n} \left[\left(\frac{u}{\sqrt{n}}, \frac{v}{\sqrt{n}} \right) - (u_0, v_0) \right]$$

corresponds to the quantities which appear in the n -th random point (1.8).

The reader may wonder about some conceptual interpretation of the somewhat mysterious formula for the variance (1.10). We hope this a good motivation for continuing reading because Conjecture 1.5 seems to be a special case of a more general result (Theorem 2.3).

Remark 1.6. It would be interesting to compare Conjecture 1.5 to the results of some Monte Carlo experiments by Vassiliev, Duzhin, and Kuzmin [VDK19]. Note, however, that some of their results seem to be based on corrupted data. For example, the plots on [VDK19, Figure 8] fail to have the axial symmetry with respect to the axis $W = 0$, respectively the central symmetry around $W = 0$ and $\mu = \frac{1}{2}$. These symmetries should be present because (with the notations of Conjecture 1.5) they correspond to replacing the numbers z, w_1, w_2, \dots by $1 - z, 1 - w_1, 1 - w_2, \dots$; such a replacement changes the shape of the corresponding RSK diagram to its transpose.

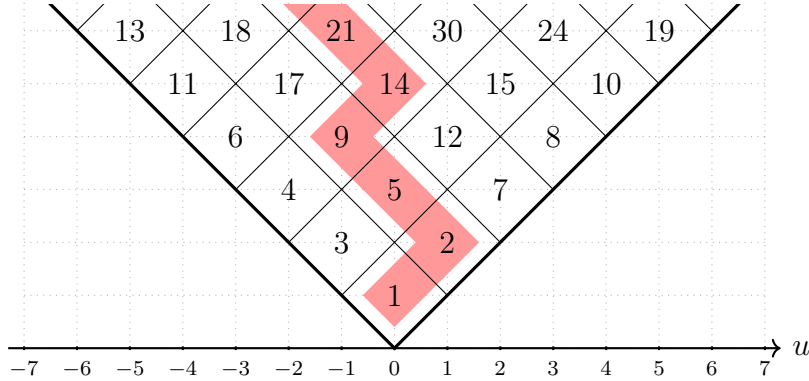


Figure 7. A part of an infinite Young tableau drawn in the Russian coordinate system. The highlighted boxes form the beginning of the jeu de taquin path.

1.6. Jeu de taquin trajectories. Given an infinite Young tableau T we view it in the Russian coordinate system, see Figure 7. We define an infinite lattice path as follows: one starts from the corner box of the tableau and keeps traveling in unit steps north-south or north-east, at each step choosing the direction among the two in which the entry in the tableau is smaller. We refer to the path defined in this way as the *jeu de taquin path* of the tableau T . This is illustrated in Figure 7. For an integer $n \geq 1$ let $j_n = j_n(T) = (u_n, v_n) \in \mathbb{Z}^2$ be the last box in the jeu de taquin path of T which contains a number $\leq n$. We refer to the sequence (j_n) as the *jeu de taquin path in the lazy parametrization* (in the Russian coordinate system).

We conjecture that the following analogue of Donsker's functional central limit theorem holds true for jeu de taquin paths. This claim is a refinement of [RS15, Theorem 5.2].

Conjecture 1.7 (The second main conjecture). *Let $z \in [0, 1]$ be fixed and let w_1, w_2, \dots be a sequence of independent, identically distributed random variables with the uniform distribution $U(0, 1)$ on the unit interval. Let $T = Q_\infty(1 - z, w_1, w_2, \dots)$ be the corresponding random infinite recording tableau. and let j_1, j_2, \dots be the corresponding jeu de taquin path in the tableau T in the lazy parametrization.*

As $c \rightarrow \infty$, the random function

$$(1.11) \quad \mathbb{R}_+ \ni t \mapsto \sqrt[4]{c} \left[\frac{1}{\sqrt{c}} j_{\lceil ct^2 \rceil} - (tu_0, tv_0) \right] \in \mathbb{R}^2$$

converges in distribution to the two-dimensional Brownian motion (U_t, V_t) which is supported on the line (1.9) and for which the covariance of the

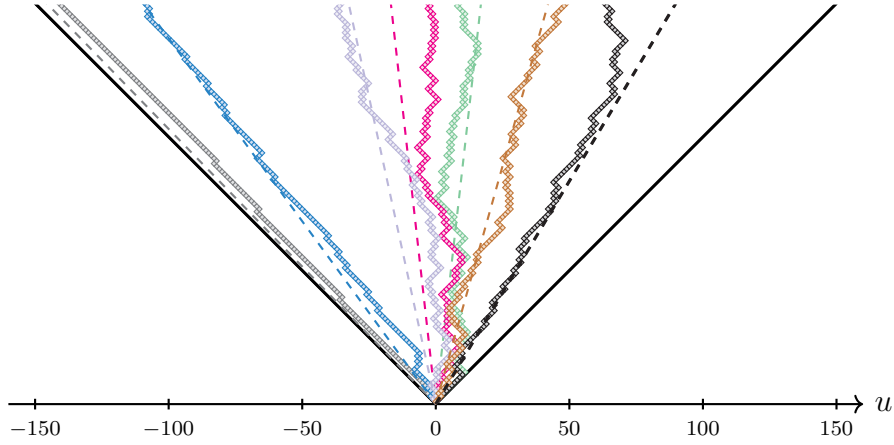


Figure 8. Several simulated paths of jeu de taquin and (dashed lines) their asymptotes. Figure excerpted from [RS15].

u -coordinates is given by

$$\mathbb{E}U_t U_s = \min(t, s) \sigma_{u_0}^2,$$

where the constant σ_{u_0} is given by (1.10).

A special case of Conjecture 1.5 for $z = \frac{1}{2}$ was conjectured by Wojtyniak [Woj19] (with a slightly different form of the variance (1.10)) based on extensive Monte Carlo simulations.

Conjecture 1.7 would imply Conjecture 1.5; indeed, one of the consequences of Conjecture 1.7 is the information about the limit distribution of the random function (1.11) evaluated at the fixed time $t = 1$. Fairly standard methods allow to relate this probability distribution to the one from Conjecture 1.5, see [RS15, Section 5.2].

1.7. Second class particles. With the notations of Conjecture 1.7, if z is assumed to be random, with the uniform distribution $U(0, 1)$ then the recording tableau T is a Plancherel-distributed infinite standard Young tableau which, thanks to Rost's map [Ros81], can be seen as *Plancherel-TASEP interacting particle system* [RS15, Section 7]. In this language, the u -coordinate u_n of the jeu de taquin box j_n can be seen as the position of *the second class particle* in this interacting particle system at time n . In this way a part of Conjecture 1.7 can be reformulated as follows.

Conjecture 1.8. *Consider Plancherel-TASEP interacting particle system and let j_n be the position of the second class particle after n steps. There*

exists a random variable V with the semicircle distribution μ_{SC} on the interval $[-2, 2]$ such that the random function

$$\mathbb{R}_+ \ni t \mapsto \frac{\sqrt[4]{c}}{\sigma_V} \left[\frac{u_{\lfloor ct^2 \rfloor}}{\sqrt{c}} - Vt \right]$$

converges in distribution to the standard Brownian motion $B(t)$ as $c \rightarrow \infty$.

For the random variable $V = F_{\text{SC}}^{-1}(z)$ one can take the appropriate quantile of the semicircle distribution.

Heuristically, this conjecture says that asymptotically the second class particles follows a drift with the random velocity V plus a (rescaled) Brownian motion and the approximate equality

$$u_{\lfloor t^2 \rfloor} \approx Vt + \sigma_V B(t)$$

holds true for $t \rightarrow \infty$; in particular the fluctuations are of order $t^{\frac{1}{2}}$. It would be interesting to explore the links of this conjecture with analogous results which are available for the usual TASEP model and the competition interface [FMP09; RV21]. It *seems* that the corresponding fluctuations are superdiffusive, of order $t^{\frac{2}{3}}$, however we are not aware of a definitive, rigorous treatment of this topic in the literature.

1.8. Overview of the paper. The setup considered in Conjecture 1.5 is probably the most natural concrete incarnation of the general problem of understanding the position of the new box when a deterministic number z is inserted into a random tableau T ; in this setup the tableau $T = P(w_1, \dots, w_n)$ is the insertion tableau corresponding to a sequence of i.i.d. random variables. Regretfully, the complete proof of this conjecture is currently beyond our reach.

In Section 2 we will consider another setup in which a deterministic number z is inserted into a *random tableau of fixed shape* (see Section 2.3 for the details). Our main result is Theorem 2.3 which can be regarded as an analogue of Conjecture 1.5. The remaining part of the paper is a preparation for the proof of Theorem 2.3.

In Section 3 we introduce our main tool: the *cumulative function* $u \mapsto F_T(u)$ which for a given tableau T gives, roughly speaking, the relationship between the location of the new box (encoded by the real number u) and the value of the inserted number. Our main technical tool is Theorem 3.2 which gives a convenient explicit combinatorial formula for the cumulants of the random variable $F_T(u_0)$ if T is a uniformly random tableau with a given shape. The proof of Theorem 3.2 is postponed to Sections 6 to 9.

In Section 4 we explore the easiest consequences of the aforementioned formula for the cumulants of the cumulative function. The key observation is that in many asymptotic setups it implies an upper bound for the

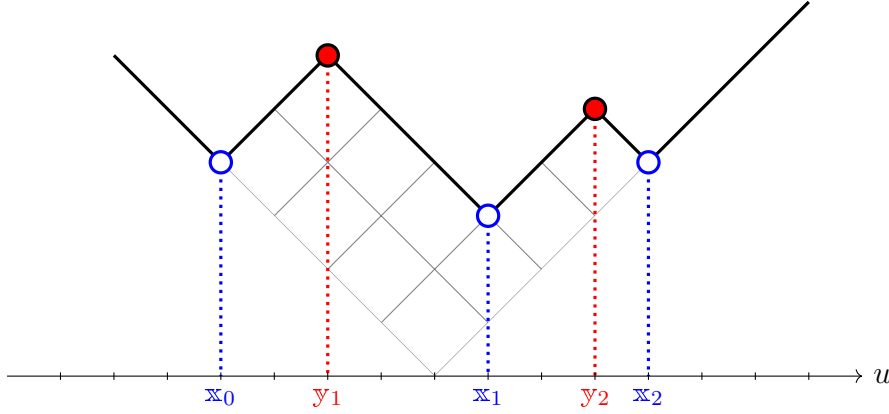


Figure 9. Concave corners (empty) and convex corners (filled) of a Young diagram $(4, 2, 2, 2)$ and their u -coordinates.

cumulants; as a consequence the random variable $F_T(u_0)$ can be well approximated by a normal distribution. Since for some special choice of u_0 the random variable $F_T(u_0)$ has a very direct interpretation as the last (i.e., rightmost) box in the bottom row of the tableau T , the latter converges in distribution towards a normal distribution, see Corollary 4.1 for the details.

Basing on these ideas, in Section 5 we complete the proof of Theorem 2.3.

Sections 6 to 9 contain the proof of Theorem 3.2.

2. THE GENERAL FORM OF RSK INSERTION FLUCTUATIONS

2.1. Plancherel growth process. Let w_1, w_2, \dots be a sequence of i.i.d. random variables with the uniform distribution $U(0, 1)$. Let

$$\lambda^{(n)} := \text{RSK}(w_1, \dots, w_n);$$

we say that the random sequence of Young diagrams

$$(2.1) \quad \emptyset = \lambda^{(0)} \nearrow \lambda^{(1)} \nearrow \dots$$

is the *Plancherel growth process* [Rom15, Chapter 1.19]. It turns out that (2.1) is a Markov chain; below we will describe its transition probabilities.

Note that the above construction is a specific case of a more general setup which we already discussed in Section 1.2.2.

2.2. Transition measure of a Young diagram. For a given Young diagram λ with n boxes we denote by $x_0 < \dots < x_L$ the u -coordinates of its concave corners and by $y_1 < \dots < y_L$ the u -coordinates of its *convex*

corners, see Figure 9. The *Cauchy transform* of λ is defined as the rational function (see [Ker93] and [Ker03, Chapter 4, Section 1])

$$(2.2) \quad \mathbf{G}_\lambda(z) = \frac{(z - \mathbb{Y}_1) \cdots (z - \mathbb{Y}_\mathbb{L})}{(z - \mathbb{X}_0) \cdots (z - \mathbb{X}_\mathbb{L})}.$$

The Cauchy transform can be written as a sum of simple fractions:

$$\mathbf{G}_\lambda(z) = \sum_{0 \leq i \leq \mathbb{L}} \frac{p_i}{z - \mathbb{X}_i}$$

with the coefficients $p_0, \dots, p_\mathbb{L} > 0$ such that $p_0 + \dots + p_\mathbb{L} = 1$. We define the *transition measure* of λ as the discrete measure

$$\mu_\lambda = p_0 \delta_{\mathbb{X}_0} + \dots + p_\mathbb{L} \delta_{\mathbb{X}_\mathbb{L}};$$

in this way

$$\mathbf{G}_\lambda(z) = \int_{\mathbb{R}} \frac{1}{z - x} d\mu_\lambda(x)$$

is indeed the Cauchy transform of μ_λ .

Kerov proved that the transition probabilities of the Markov chain (2.1) are encoded by the transition measure, see [Ker93] and [Ker03, Chapter 4, Section 1]. More specifically, the conditional probability that the new box will have the u -coordinate equal to \mathbb{X}_i is given by

$$(2.3) \quad \mathbb{P} \left[u \left(\lambda^{(n+1)} \setminus \lambda^{(n)} \right) = \mathbb{X}_i \mid \lambda^{(n)} = \lambda \right] = p_i = \text{Res}_{\mathbb{X}_i} \mathbf{G}_\lambda,$$

i.e., by the corresponding atom of the transition measure as well as by the residue of the Cauchy transform.

We denote by

$$(2.4) \quad K_\lambda(z) = \mu_\lambda((-\infty, z])$$

the cumulative distribution function of μ_λ .

2.3. Random Poissonized tableau of a given shape. By a *Poissonized tableau* [GR19] we mean any tableau which has the real numbers from the unit interval $[0, 1]$ as the entries. The set of Poissonized tableaux with shape λ will be denoted by \mathcal{T}^λ . There are two natural ways to equip \mathcal{T}^λ with a probability measure, we will discuss them below.

Firstly, let us number the boxes of λ in an arbitrary way; it follows that each element of \mathcal{T}^λ can be identified with an element of the unit cube $[0, 1]^n$, where n is the number of boxes of λ . The requirement that the rows and the columns are increasing corresponds to a collection of inequalities between the coordinates of the points in the cube; it follows that \mathcal{T}^λ can be identified with a convex polytope contained in $[0, 1]^n$. This polytope has a strictly positive volume therefore it is possible to equip it with the *uniform probability measure*.

On the other hand, the canonical way of generating a random Poissonized tableau T with a prescribed number of boxes n is to consider the insertion tableau $P(w)$, where $w = (w_1, \dots, w_n)$ is a sequence of i.i.d. random numbers with the $U(0, 1)$ distribution. If we condition the random tableau T so that its shape is equal to λ , it becomes a natural candidate for the notion of a *uniformly random Poissonized tableau of shape λ* .

The following lemma shows that the above two approaches give rise to the same probability distribution.

Lemma 2.1. *Let $w = (w_1, \dots, w_n)$ be a sequence of i.i.d. random variables with the $U(0, 1)$ distribution and let λ be a Young diagram with n boxes.*

The conditional probability distribution of the insertion tableau $P(w)$ under the condition that $\text{RSK}(w) = \lambda$ coincides with the uniform probability distribution on \mathcal{T}^λ .

The proof is postponed to Section 6.1.

2.4. Asymptotic determinism of Schensted insertion. We start with the following generalization of the result of Romik and the second named author (Theorem 1.4). Recall that K_λ is the cumulative distribution function of the transition measure μ_λ , see (2.4).

Theorem 2.2. *For each n let $\lambda^{(n)}$ be a random Young diagram with n boxes. We assume that there is a probability measure ν on the real line such that for each $u \in \mathbb{R}$ for which the cumulative distribution function F_ν is continuous, the limit*

$$K_{\lambda^{(n)}}(\sqrt{n} u) \xrightarrow[n \rightarrow \infty]{P} F_\nu(u)$$

holds true in probability.

Assume that $0 < z < 1$ is such that the quantile function F_ν^{-1} is continuous in z ; we set $u_0 = F_\nu^{-1}(z)$. Then

$$\frac{1}{\sqrt{n}} \text{u-Ins}(T^{(n)}; z) \xrightarrow[n \rightarrow \infty]{P} u_0$$

In particular, Theorem 2.2 combined with Theorem 1.3 provides a conceptually new proof of Theorem 1.4.

The proof of Theorem 2.2 is postponed to Section 5.3.

2.5. The interaction energy. If μ is a probability measure on the real line and $u_0 \in \mathbb{R}$ we define

$$(2.5) \quad \mathcal{E}_\mu(u_0) = \iint_{\{(z_1, z_2): z_1 < u_0 < z_2\}} \frac{1}{z_2 - z_1} d\mu(z_1) d\mu(z_2)$$

whenever this double integral is finite. This quantity will play an important role in the statement of our main result.

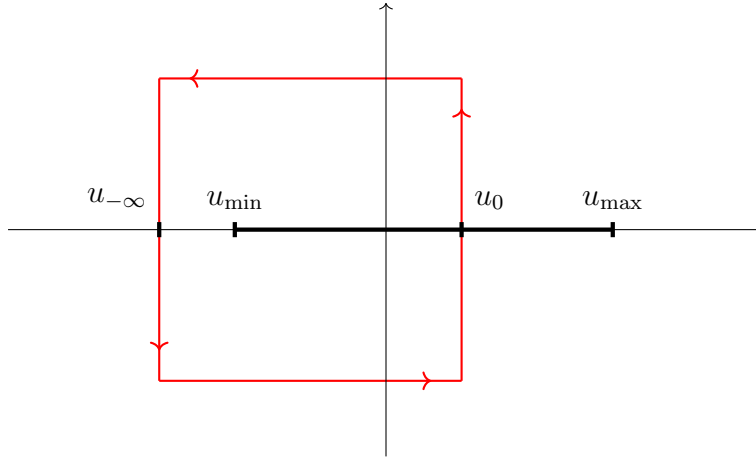


Figure 10. The contour C on the complex plane.

Let us interpret μ as the distribution of the electrostatic charge along a one-dimensional rod. If we split this rod at the point u_0 , the two parts will act on one another with the electrostatic force. The integral (2.5) can be interpreted as the *interaction energy* between these two parts.

We now consider an alternative universe in which the space is two-dimensional so that the electrostatic force decays as the inverse of the distance between the charges. It follows that the double integral $\mathcal{E}_\mu(u_0)$ is equal to the *electrostatic force* between the two parts of the rod.

If we separate the two parts of the rod by an additional distance l , the aforementioned electrostatic force is the derivative of the total energy of the system with respect to the variable l . It is worth pointing out that in our context *the total energy* should be understood as the logarithmic energy which is ubiquitous in random matrix theory, Voiculescu's free entropy [Voi94], as well as in asymptotic representation theory. For this reason we suspect that the interaction energy $\mathcal{E}_\mu(u_0)$ can be found also in the context of random matrix theory.

Suppose that the support of the measure μ is contained in some interval $[u_{\min}, u_{\max}]$. We choose an arbitrary real number $u_{-\infty}$ such that $u_{-\infty} < u_{\min}$ and consider a contour C on the complex plane shown in Figure 10. This contour was chosen in such a way that it crosses the real line in two points, namely, $u_{-\infty}$ and u_0 .

In the special case when the support of μ is a finite set and u_0 does not belong to the support of μ we may apply Cauchy's residue theorem and the

interaction energy is equal to the contour integral

$$(2.6) \quad \mathcal{E}_\mu(u_0) = -\frac{1}{4\pi i} \oint_C [\mathbf{G}_\mu(z)]^2 dz,$$

where

$$\mathbf{G}_\mu(z) = \int_{\mathbb{R}} \frac{1}{z - x} d\mu(x)$$

is the Cauchy transform of μ . The formula (2.6) remains true for general measures μ as long as the Cauchy transform is sufficiently regular in the neighborhood of u_0 , however the justification of its validity is more technically involved. In practical applications the formula (2.6) is more convenient than (2.5).

We define also

$$\mathbf{G}_\mu^+(z) = \int_{\mathbb{R}} \frac{1}{|z - x| + 1} d\mu(x)$$

as a (slightly regularized) version of the Cauchy transform with the absolute value of the original kernel. For a Young diagram λ we will use the simplified notation

$$\mathbf{G}_\lambda^+ = \mathbf{G}_{\mu_\lambda}^+.$$

2.6. General form of the fluctuations. Recall that K_λ is the cumulative distribution function of the transition measure μ_λ , see (2.4).

Theorem 2.3 (The main theorem). *Let $u_0 \in \mathbb{R}$, $0 < z < 1$, $f > 0$, and $\mathcal{E} > 0$ be fixed. For each integer $n \geq 1$ let $\lambda^{(n)}$ be a random Young diagram. We assume that*

(a) *for each $c \in \mathbb{R}$*

$$\sqrt[4]{n} \left\{ K_{\lambda^{(n)}} \left[\sqrt{n} \left(u_0 + \frac{c}{\sqrt[4]{n}} \right) \right] - \left[z + f \frac{c}{\sqrt[4]{n}} \right] \right\} \xrightarrow[n \rightarrow \infty]{P} 0,$$

(b) *for each $c \in \mathbb{R}$*

$$(2.7) \quad \sqrt{n} \sum_{\substack{x_1 \leq \sqrt{n} u + \sqrt[4]{n} c, \\ x_2 > \sqrt{n} u + \sqrt[4]{n} c}} \frac{1}{x_2 - x_1 + 1} \mu_{\lambda^{(n)}}(x_1) \mu_{\lambda^{(n)}}(x_2) \xrightarrow[n \rightarrow \infty]{P} \mathcal{E},$$

(c) *for each $c \in \mathbb{R}$ there exists an exponent $\alpha \geq \frac{3}{8}$ such that*

$$(2.8) \quad n^\alpha \mathbf{G}_{\lambda^{(n)}}^+ \left[\sqrt{n} \left(u_0 + \frac{c}{\sqrt[4]{n}} \right) \right] \xrightarrow[n \rightarrow \infty]{P} 0.$$

Let $T^{(n)}$ be a uniformly random Poissonized tableau of shape $\lambda^{(n)}$. Then

$$(2.9) \quad \sqrt[4]{n} \left[\frac{\text{u-Ins}(T^{(n)}; z)}{\sqrt{n}} - u_0 \right] \xrightarrow[n \rightarrow \infty]{\text{dist}} N \left(0, \frac{\mathcal{E}}{f^2} \right).$$

In a typical application the rescaled shapes of the Young diagrams $\lambda^{(n)}$ converge to some limit curve which, roughly speaking, means that the (diluted by factor $n^{-\frac{1}{2}}$) Kerov's transition measure of $\lambda^{(n)}$ converges in the weak topology of probability measures to some probability measure μ on the real line. In this context the condition (a) can be replaced by the stronger assumption that the conjunction of the following conditions holds true:

(a1) for each $u \in \mathbb{R}$

$$K_{\lambda^{(n)}}(\sqrt{n} u) \xrightarrow[n \rightarrow \infty]{P} F_\mu(u),$$

where F_μ is the cumulative distribution function of the probability measure μ ;

(a2) there exists an open neighborhood U of u_0 such that for each $\epsilon > 0$

$$\sup_{u \in U} \mathbb{P} \left(\left| K_{\lambda^{(n)}}(\sqrt{n} u) - F_\mu(u) \right| > \frac{\epsilon}{\sqrt[4]{n}} \right) \xrightarrow[n \rightarrow \infty]{} 0,$$

(a3) the measure μ in u_0 has density equal to

$$f = F'_\mu(u_0).$$

In the above scenario the (lower) limit of the expression on the left-hand side is bounded *from below* by the interaction energy $\mathcal{E}_\mu(u_0)$ of the limit measure thus $\mathcal{E} \geq \mathcal{E}_\mu(u_0)$. We conjecture that in *nice* examples (under some additional technical assumptions?) the above assumptions would imply that the condition (b) holds true with

$$\mathcal{E} = \mathcal{E}_\mu(u_0).$$

Note that the left-hand side of (2.7), regarded as a function of c , converges to $c \mapsto \mathcal{E}_\mu(c)$ in the $L^1(A, B)$ norm for any $A < B$ so for a *typical* value of c the condition (a2) seems to imply (b).

For any probability measure ν on the real line and any $A < B$

$$\int_A^B \mathbf{G}_\nu^+(\sqrt{n} x) dx \leq \frac{2}{\sqrt{n}} \log [(B - A)\sqrt{n} + 1]$$

thus the left-hand side of (2.8), viewed as a function of c , converges to zero in the $L^1[A, B]$ norm on the interval $[A, B]$ as long as $\alpha < 1$. Again, for a *typical* value of c we may hope that the condition 2.8 is fulfilled.

The proof of Theorem 2.3 is postponed to Section 5.

2.7. Example: staircase tableaux. In Theorem 2.3 we will pass to a subsequence defined as

$$n = n_N = 1 + \cdots + N = \frac{N(N+1)}{2}.$$

We define

$$(2.10) \quad \lambda^{(n_N)} = (N, N-1, \dots, 3, 2, 1)$$

to be a *staircase Young diagram* with n_N boxes. A straightforward calculation of the residues of the Cauchy transform shows that the transition measure of $\lambda^{(n)}$ is supported on the set of even, respectively odd numbers

$$\{-N, -N+2, \dots, N-2, N\}$$

with the probabilities

$$(2.11) \quad \mu_{\lambda^{(n)}}(2k-N) = \frac{1}{2^{2k}} \binom{2k}{k} \binom{2N-2k}{N-k}$$

for $k \in \{0, \dots, N\}$. This probability distribution appears naturally in the context of random walks and the *arcsine theorem*, see [Fel68, Chapter III]. The limit measure μ_{AS} of the dilated measures $D_{\frac{1}{\sqrt{n}}} \mu_{\lambda^{(n)}}$ is the arcsine law supported on the interval $I = [-\sqrt{2}, \sqrt{2}]$ with the density

$$f_{AS}(z) = \frac{1}{\pi \sqrt{2-z^2}} \quad \text{for } z \in I.$$

It is easy to verify (for example, by the Stieltjes inversion formula) that the Cauchy transform of this measure is given by

$$\mathbf{G}_{AS}(z) = \frac{1}{\sqrt{z^2-2}} \quad \text{for } z \in \mathbb{C} \setminus I.$$

The formula (2.6) implies therefore that if $-\sqrt{2} < u_0 < \sqrt{2}$ then the value of $(-2)\mathcal{E}_{AS}(u_0)$ is equal to the residue of the function $z \mapsto \frac{1}{z^2-2}$ in $z = -\sqrt{2}$. In this way we get that the interaction energy of the arcsine measure is given by

$$(2.12) \quad \mathcal{E}_{AS}(u_0) = \begin{cases} 0 & \text{if } u_0 < -\sqrt{2}, \\ \frac{1}{4\sqrt{2}} & \text{if } -\sqrt{2} < u_0 < \sqrt{2}, \\ 0 & \text{if } u_0 > \sqrt{2}. \end{cases}$$

Corollary 2.4. *Let $0 < z < 1$ be fixed and let $u_0 = F_{AS}^{-1}(z)$ be the corresponding quantile of the arcsine distribution. For each n of the form $n = n_M$ let $T^{(n)}$ be a uniformly random Poissonized tableau of the staircase shape.*

Then the sequence of random variables

$$\sqrt[4]{n} \left[\frac{1}{\sqrt{n}} \text{u-Ins} \left(T^{(n)}; z \right) - u_0 \right] \xrightarrow{\text{dist}} N(0, \sigma_{\text{AS}}^2(u_0))$$

converges in distribution to the centered Gaussian measure with the variance

$$\sigma_{\text{AS}}^2(u_0) = \frac{\pi^2}{4\sqrt{2}}(2 - u_0^2).$$

Proof. It is enough to verify that the assumptions of Theorem 2.3 are fulfilled. A small refinement of the calculation from [Fel68, Chapter III] gives more precise asymptotics of the probabilities (2.11); as a consequence we get that for each $\epsilon > 0$

$$\sup_{-\sqrt{2}+\epsilon < z < \sqrt{2}-\epsilon} \left| K_{\lambda^{(n)}}(\sqrt{n} z) - F_{\text{SC}}(z) \right| = O\left(\frac{1}{\sqrt{n}}\right) \ll O\left(\frac{1}{\sqrt[4]{n}}\right)$$

which implies that the conditions (a1) and (a2) are satisfied; the condition (a3) is clearly satisfied.

The aforementioned asymptotics of the probabilities (2.11) combined with elementary calculus imply that condition (b) holds true with $\mathcal{E} = \mathcal{E}_{\text{SC}}(u_0)$ equal to the interaction energy of the semicircle measure. Also, for each $\epsilon > 0$

$$\sup_{-\sqrt{2}+\epsilon < z < \sqrt{2}-\epsilon} \mathbf{G}_{\lambda^{(n)}}^+(\sqrt{n} z) = O\left(\frac{\log n}{\sqrt{n}}\right)$$

which shows that the condition (c) holds true for each $\alpha < \frac{1}{2}$. \square

We will revisit this example in Section 5.2.

2.8. Towards Conjecture 1.5. Our strategy towards the proof of Conjecture 1.5 is to apply Theorem 2.3 with a specific choice of the measure $\mu = \mu_{\text{SC}}$ given by the semicircle distribution considered in Section 1.4.3. It seems that the key difficulty is to verify that some version of the assumption (a) from Theorem 2.3 holds true.

Our Monte Carlo experiments (such as the plots of the red thin curve on Figures 12 and 13) as well as some educated guesses based on the counterparts in the random matrix theory [Gus05] suggest that the following much stronger result holds true.

Conjecture 2.5. *Let $\lambda^{(n)}$ be a random Young diagram with n boxes distributed according to the Plancherel measure. For each $-2 < u < 2$ and each $\alpha < \frac{1}{2}$*

$$n^\alpha \left[K_{\lambda^{(n)}}(\sqrt{n} u) - F_{\text{SC}}(u) \right] \xrightarrow[n \rightarrow \infty]{P} 0.$$

The case $\alpha = 0$ clearly holds true since it corresponds the usual weak convergence of probability measures [RS15, Theorem 3.2]. It seems even a quite suboptimal case $\alpha = \frac{1}{4}$ (with some locally uniform bounds on the rate of decay of the probability of a error larger than given $\epsilon > 0$) would be enough to guarantee that the condition (a) from Theorem 2.3 holds true. We expect that the proof of Conjecture 2.5, as a side product, would give some regularity results which guarantee that the remaining assumptions of Theorem 2.3 are fulfilled as well. Unfortunately, Conjecture 2.5 is currently beyond our reach.

Proposition 2.6. *For the semicircle measure μ_{SC} the corresponding interaction energy is given by*

$$\mathcal{E}_{\text{SC}}(u) = \begin{cases} \frac{1}{12\pi} (4 - u^2)^{\frac{3}{2}} & \text{for } -2 \leq u \leq 2, \\ 0 & \text{otherwise.} \end{cases}$$

Proof. The method of the contour integral considered in Section 2.5 is applicable; we leave the details for the interested reader. In the following we provide an alternative method.

For $\epsilon \in \mathbb{R}$ we define the regularized version of $\mathcal{E}_{\text{SC}}(u)$ given by

$$\mathcal{E}_\epsilon(u) := \iint_{-2 < z_1 < u < z_2 < 2} \Re \frac{1}{z_2 - z_1 + i\epsilon} f_{\text{SC}}(z_1) f_{\text{SC}}(z_2) dz_1 dz_2;$$

our goal is to evaluate $\mathcal{E}_0(u) = \mathcal{E}_{\text{SC}}(u)$. Note that for real numbers $z_2 > z_1$

$$\mathbb{R}_+ \ni \epsilon \mapsto \Re \frac{1}{z_2 - z_1 + i\epsilon} = \frac{z_2 - z_1}{(z_2 - z_1)^2 + \epsilon^2}$$

is a decreasing, positive, continuous function. By Lebesgue monotone convergence theorem it follows that

$$F_0(u) = \lim_{\epsilon \rightarrow 0} F_\epsilon(u).$$

In order to evaluate $F_\epsilon(u)$ we notice that for $\epsilon > 0$ the derivative of \mathcal{E}_ϵ is given by

$$\begin{aligned} \mathcal{E}'_\epsilon(u) &= \int_{u < z_2 < 2} \Re \frac{1}{z_2 - u + i\epsilon} f_{\text{SC}}(u) f_{\text{SC}}(z_2) dz_2 - \\ &\quad \int_{-2 < z_1 < u} \Re \frac{1}{u - z_1 + i\epsilon} f_{\text{SC}}(z_1) f_{\text{SC}}(u) dz_1 = \\ &= f_{\text{SC}}(u) \Re \int_{-2 < z < 2} \frac{1}{z - (u + i\epsilon)} f_{\text{SC}}(z) dz = \\ &= f_{\text{SC}}(u) \Re \mathbf{G}_{\text{SC}}(u + i\epsilon); \end{aligned}$$

above we used the fact that the integral on the right-hand side is the Cauchy transform of the semicircular distribution

$$\mathbf{G}_{\text{SC}}(w) = \int_{-2 < z < 2} \frac{1}{z - w} f_{\text{SC}}(z) dz = \frac{-w + \sqrt{w^2 - 4}}{2},$$

evaluated at $w = i + i\epsilon$, see [MS17, Section 3.1]

For $-2 \leq u \leq 2$ the principal value of the Cauchy integral is given by

$$\mathbf{G}_{\text{SC}}(u) = \lim_{\epsilon \rightarrow 0} \Re \mathbf{G}_{\text{SC}}(u + i\epsilon) = -\frac{u}{2}$$

and the convergence is uniform over the interval $[-2, 2]$. We proved in this way that

$$(2.13) \quad \mathcal{E}'_{\text{SC}}(u) = f_{\text{SC}}(u) \mathbf{G}_{\text{SC}}(u).$$

It follows that

$$\mathcal{E}_{\text{SC}}(u) = \int_{-2}^u f_{\text{SC}}(w) \frac{-w}{2} dw = \frac{1}{12\pi} (4 - u^2)^{\frac{3}{2}} \quad \text{for } -2 \leq u \leq 2.$$

The above calculation can be generalized to other measures than the semicircular law for which the Cauchy transform is sufficiently regular. Be warned, that for the example of the arc-sine law from Section 2.7 the analogue of (2.13) implies that

$$\mathcal{E}'_{\text{AS}}(u) = 0$$

which, technically speaking is correct, but not very helpful for finding the exact form of the formula (2.12). \square

Our choice of the variance (1.10) in Conjecture 1.5 is equal to $\frac{\mathcal{E}_{\text{SC}}}{(f_{\text{SC}})^2}$ and it was based on the the variance on the right-hand side of (2.9).

3. THE KEY TOOL:

THE CUMULATIVE FUNCTION OF A TABLEAU AND ITS CUMULANTS

3.1. The cumulative function of a tableau. Let T be a Poissonized tableau. For $u_0 \in \mathbb{R}$ we define

$$F_T(u_0) = \inf \{z \in [0, 1] : \text{u-Ins}(T; z) \geq u_0\};$$

we recall that the quantity $\text{u-Ins}(T; z)$ was defined in Section 1.3 as the u -coordinate of the box $\text{Ins}(T; z)$. In the case when the infimum runs over the empty set, we declare that $F_T(u_0) = 1$, see Figure 11 for an example. From the monotonicity of the Schensted row insertion it follows that

$$(3.1) \quad F_T(u_0) \leq z \iff \text{u-Ins}(T; z) \geq u_0$$

holds true for any $u_0 \in \mathbb{R}$ and $z \in [0, 1]$.

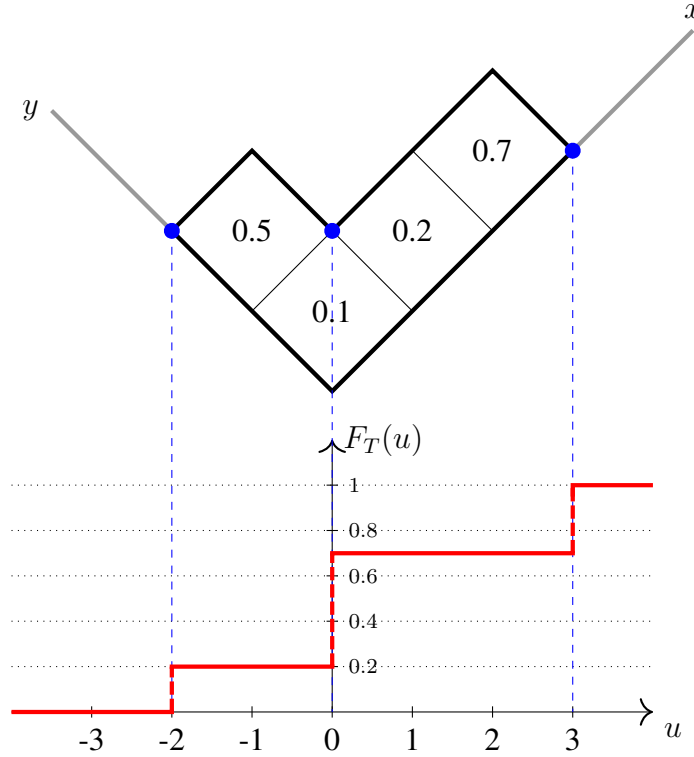


Figure 11. A Poissonized tableau T shown in the Russian coordinates. The red line depicts its cumulative function F_T .

The function $F_T: \mathbb{R} \rightarrow [0, 1]$ will be called *the cumulative function of T* . It has analogous properties as any cumulative distribution function of a probability measure with a finite support. It can be regarded as an inverse of the insertion function $z \mapsto \text{u-Ins}(T; z)$; more precisely the relationship between F_T and $\text{u-Ins}(T; \cdot)$ is the same as between the cumulative distribution function of a measure and the quantile function.

This relationship is the key motivation for studying the cumulative function F_T . Indeed, since Conjecture 1.5 and Theorem 2.3 can be seen as limit statements about the probability distribution of the (random) function

$$z \mapsto \text{u-Ins}(T; z)$$

for some special choices for the random tableau T , a natural direction for proving these results is to prove suitable limit results for its inverse function F_T .

3.2. Asymptotics of the cumulative function of random tableaux. Let us choose somehow (randomly or deterministically) a Young diagram λ ,

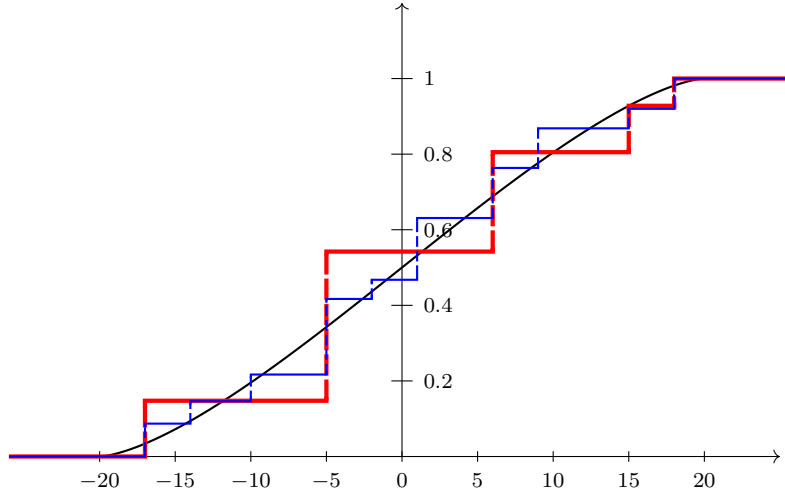


Figure 12. The insertion tableau $T = P(w_1, \dots, w_n)$ with $n = 100$ boxes was sampled by applying the RSK algorithm to a sequence of i.i.d. $U(0, 1)$ random variables. The thin blue line shows the cumulative distribution function K_λ of the transition measure of the shape λ of T . The thick red line shows the cumulative function F_T . The smooth black line is the cumulative distribution function of the semicircle distribution supported on the interval $[-2\sqrt{n}, 2\sqrt{n}]$.

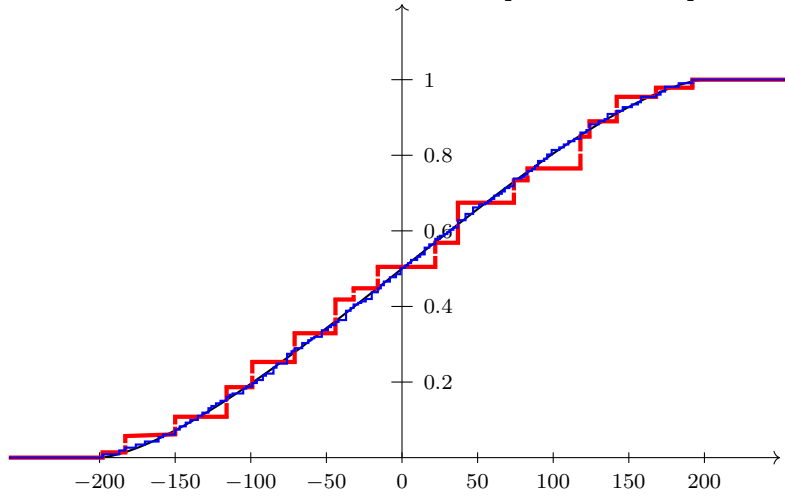


Figure 13. An analogue of Figure 12 for $n = 10^4$.

and let T be a random Poissonized tableau of shape λ . It is a very interesting problem to study the asymptotics of the random function $u_0 \mapsto F_T(u_0)$,

in the limit as the number of boxes of λ tends to infinity. The main technical tool of the current paper (Theorem 3.2) is an answer to the following more modest problem related to the *pointwise* behavior of the cumulative function.

Problem 3.1. *Let λ be Young diagram and let T be a uniformly random normalized tableau with shape λ . For a given $u_0 \in \mathbb{R}$ find the probability distribution of the random variable $F_T(u_0)$.*

A concrete version of this general problem is to take λ to be a Plancherel-distributed random Young diagram with n boxes. The resulting random tableau T can be then alternatively generated as the insertion tableau $T = P(w_1, \dots, w_n)$ corresponding to a sequence of i.i.d. $U(0, 1)$ random variables, see Lemma 2.1. The simulations on Figures 12 and 13 show (i) the cumulative function F_T (the thick red line), as well as (ii) the cumulative distribution function K_λ of the transition measure of λ , in relation to (iii) the cumulative distribution function of the rescaled arc-sine law (the smooth black line). It is not very surprising that the curves (i) and (ii) become closer and closer to the curve (iii) as the size $n \rightarrow \infty$ of the Young diagram tends to infinity; for the curve (ii) it is a classical result (see [RS15, Theorem 3.2]) and for the curve (i) it is reformulation of Theorem 1.4 as well as a special case of Theorem 2.2. The surprising feature of these plots is that the rate of convergence in the case (i) seems to be of order $\Theta\left(n^{-\frac{1}{4}}\right)$ (to some extent this rate of convergence can be justified by the proof of Theorem 2.3 in Section 5.4) while in the case (ii) the analogous rate of convergence seems to be of much smaller order $O\left(n^{-\frac{1}{2}+\epsilon}\right)$, see Conjecture 2.5.

3.3. Cumulants and moments. Let X be a random variable with the sequence of moments $(m_k)_{k=1}^\infty$, where $m_k = \mathbb{E}X^k$. The formal power series

$$\mathbb{E}[e^{tX}] = \sum_{k=0}^{\infty} \frac{m_k}{k!} t^k$$

is its exponential moment generating function or *formal Fourier–Laplace transform*. The coefficients $(\kappa_k)_{k=1}^\infty$ of its formal logarithm

$$\log \mathbb{E}[e^{tX}] = \sum_{k=1}^{\infty} \kappa_k \frac{t^k}{k!}$$

are called the *cumulants* [LH02] of the random variable X . The first cumulant is the expected value and the second cumulant is the variance:

$$\begin{aligned} \kappa_1 &= \mathbb{E}X, \\ \kappa_2 &= \text{Var } X. \end{aligned}$$

Cumulants are related with the moments via *the moment-cumulant formula*

$$(3.2) \quad m_k = \sum_{\pi \in \Pi_k} \prod_{b \in \pi} \kappa_{|b|},$$

where the sum runs over all set-partitions π of the set $\{1, \dots, k\}$, and the product runs over all blocks of the partition π . For example, for $k = 3$ there are 5 set-partitions of the set $\{1, 2, 3\}$, namely,

$$\{\{1\}, \{2\}, \{3\}\}, \{\{1, 2\}, \{3\}\}, \{\{1, 3\}, \{2\}\}, \{\{2, 3\}, \{1\}\}, \{\{1, 2, 3\}\}.$$

Therefore

$$m_3 = \kappa_1^3 + \kappa_2 \kappa_1 + \kappa_2 \kappa_1 + \kappa_2 \kappa_1 + \kappa_3 = \kappa_1^3 + 3\kappa_2 \kappa_1 + \kappa_3.$$

3.4. Notation. By a *directed graph* we mean any graph in which every edge has been directed. The edge outgoing from the vertex a and incoming to the vertex b will be denoted by (a, b) . The directed graphs we consider do not have multiple edges, but may have *loops*, i.e., edges of the form (a, a) . We will always assume that if $a \neq b$ and (a, b) is an edge of a graph then the opposite edge (b, a) is *not* an edge.

The graphs we consider will have their vertices colored black, red, or white. For the convenience of the readers of the non-colored printed version of this paper, the red vertices will be drawn with an additional ornament as crossed-out circles, see Figure 25. For a given graph H , we denote the set of its vertices by V_H , the set of its black vertices by B_H , the set of its red vertices by R_H , the set of its white vertices by W_H , and the set of its edges by E_H .

We say that a graph is a *weighted graph* if each of its edges is assigned a number called a *weight*. For a given edge e , we denote its weight by $w(e) \in \mathbb{R}$.

3.5. Decorations. Let $\mathbb{X} \subset \mathbb{R}$ be a fixed discrete set. Also, let $u_0 \in \mathbb{R}$ be a fixed real number. The elements of the interval $(-\infty, u_0]$ will be called *small* while the elements of the interval (u_0, ∞) will be called *big*.

For a given graph H we say that a function $\mathbf{x}: V_H \rightarrow \mathbb{X}$ is a *u_0 -decoration of the graph H* if the following two conditions hold true:

$$\mathbf{x}(b) \text{ is small for each } b \in B_H,$$

$$\mathbf{x}(w) \text{ is big for each } w \in W_H.$$

For simplicity we denote $x_v = \mathbf{x}(v)$ for $v \in V_H$. The set of all u_0 -decorations of the graph H will be denoted by $D_H(u_0)$. When the value of u_0 is clear from the context, we will simply speak about *decorations* and write $D_H = D_H(u_0)$.



Figure 14. (a) The unique non-crossing alternating tree with 1 vertex. (b) The unique non-crossing alternating tree with 2 vertices.

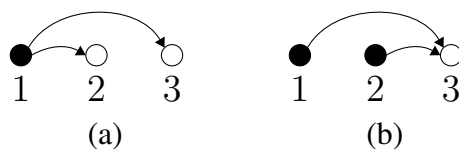


Figure 15. All non-crossing alternating trees with 3 vertices.

3.6. Non-crossing alternating trees. Let $k \geq 1$ be a natural number. We say that a tree with k vertices numbered $1, \dots, k$ is a *non-crossing alternating tree* if the following conditions hold true:

- (a) each vertex is colored either black or white;
- (b) if an edge connects the vertices b and w for $b < w$, then the vertex b is black and the vertex w is white;
- (c) there do not exist four vertices $v_1 < v_2 < v_3 < v_4$ such that v_1 is connected with v_3 , and v_2 is connected with v_4 ,

see [Sta99, Exercise 6.19(p)] and solution to this exercise, as well as [GGP97, Section 6]. The condition (c) has a natural graphical interpretation: after drawing the vertices on the real line and the edges as arcs above the real line, we require that the edges do not cross.

In the exceptional case $k = 1$ we declare that there is only one non-crossing alternating tree with 1 vertex: it consists of a single black vertex (see Figure 14a). With this convention, the condition (b) implies that the coloring of the vertices can be uniquely recovered purely from the information about the edges.

We denote by \mathbb{T}_k the set of all non-crossing alternating trees with k vertices. For example, $|\mathbb{T}_3| = 2$ (see Figure 15), and $|\mathbb{T}_4| = 5$ (see Figure 16).

In the following we will treat any non-crossing alternating tree as a directed graph in which any edge (b, w) is oriented from a black vertex and towards a white vertex; in other words from the left vertex to the right vertex.

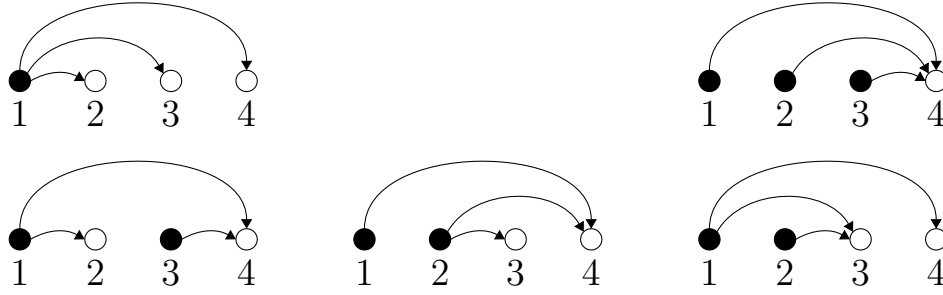


Figure 16. All non-crossing alternating trees with 4 vertices.

3.7. Closed formula for cumulants. Let λ be a fixed Young diagram. Let T be a uniformly random Poissonized tableau of shape λ , and $F_T(u_0)$ be the cumulative function of T . We will now present a closed formula for the cumulants of the random variable $F_T(u_0)$. This formula is convenient for proving that in a suitable asymptotic setting the random variable $F_T(u_0)$ (after shift and rescaling) converges in distribution towards a Gaussian measure.

Assume that the discrete set \mathbb{X} of the decoration values contains the set of u -coordinates of all concave corners of λ . In other words, we assume that the support of the transition measure of λ is contained in \mathbb{X} . For example, we may take $\mathbb{X} = \mathbb{Z}$ to be the set of integers. Note that the set $D_H(u_0)$ which is used below depends implicitly on this choice of \mathbb{X} .

Theorem 3.2. *With the above notations, for each $u_0 \in \mathbb{R}$ the k -th cumulant of the random variable $F_T(u_0)$ is given by*

$$(3.3) \quad \kappa_k(F_T(u_0)) = (k-1)! \sum_{H \in \mathbb{T}_k} \sum_{\mathbf{x} \in D_H(u_0)} \frac{(-1)^{|B_H|-1} \prod_{j=1}^k \mu_\lambda(x_j)}{\prod_{(b,w) \in E_H} (x_w - x_b + w - b)},$$

where $\mu_\lambda(x_j)$ denotes the probability corresponding to the atom x_j of the transition measure μ_λ .

The proof is contained in Sections 6 to 9.

Example 3.3. The expected value and the variance of $F_T(u_0)$ are given by

$$(3.4) \quad \mathbb{E} F_T(u_0) = \sum_{x_1 \leq u_0} \mu_\lambda(x_1),$$

$$(3.5) \quad \text{Var } F_T(u_0) = \sum_{\substack{x_1 \leq u_0 \\ x_2 > u_0}} \frac{1}{x_2 - x_1 + 1} \mu_\lambda(x_1) \mu_\lambda(x_2).$$

The unique summand on the right-hand side of (3.4) corresponds to the tree in Figure 14a, and the unique summand on the right-hand side of (3.5) corresponds to the tree in Figure 14b. The third cumulant of $F_T(u_0)$ is given by

$$\begin{aligned} k_3(F_T(u_0)) = & \sum_{\substack{x_1 \leq u_0 \\ x_2, x_3 > u_0}} \frac{2}{(x_2 - x_1 + 1)(x_3 - x_1 + 2)} \mu_\lambda(x_1) \mu_\lambda(x_2) \mu_\lambda(x_3) \\ & - \sum_{\substack{x_1, x_2 \leq u_0 \\ x_3 > u_0}} \frac{2}{(x_3 - x_2 + 1)(x_3 - x_1 + 2)} \mu_\lambda(x_1) \mu_\lambda(x_2) \mu_\lambda(x_3), \end{aligned}$$

where the first summand on the right-hand side corresponds to the tree in Figure 15a, and the second summand corresponds to the tree in Figure 15b.

Remark 3.4. The right-hand side of (3.3) can be interpreted as the expected value of the random variable Z defined in the following way. Let x_1, \dots, x_k be a sequence of independent, identically distributed random variables, with the distribution given by the transition measure μ_λ . Let $\mathbb{T}_k^\mathbf{x}$ denote the set of all trees $H \in \mathbb{T}_k$ such that $\mathbf{x} = (x_1, \dots, x_k)$ is a u_0 -decoration of the tree H , i.e., $\mathbf{x} \in D_H$. The aforementioned random variable is defined as

$$Z = (k-1)! \sum_{H \in \mathbb{T}_k^\mathbf{x}} \frac{(-1)^{|B_H|-1}}{\prod_{(b,w) \in E_H} (x_w - x_b + w - b)}.$$

3.8. Towards the proof of Theorem 3.2. Rational functions associated to a graph. Our proof of Theorem 3.2 is based on algebraic identities fulfilled by some rational multivariate functions. It turns out that the class of the rational functions which we consider is naturally indexed by oriented and weighted graphs, and the aforementioned algebraic identities have a natural combinatorial interpretation as removal of loops from the graphs.

For an oriented weighted graph H with the vertex set $V_H = \{v_1, \dots, v_t\}$, we consider the rational function

$$f_H = f_H(x_{v_1}, \dots, x_{v_t}) = \frac{1}{\prod_{e=(i,j) \in E_H} [x_j - x_i + w(e)]} \in \mathbb{Q}(x_{v_1}, \dots, x_{v_t})$$

in the variables corresponding to the vertices of H . In the following we will usually consider the special case when H has the vertex set $V_H = \{1, \dots, k\}$ so that

$$f_H = f_H(x_1, \dots, x_k) \in \mathbb{Q}(x_1, \dots, x_k).$$

For each tree $H \in \mathbb{T}_k$, we define the weight of an edge $e = (i, j) \in E_H$

$$(3.6) \quad w(e) = w(i, j) = j - i$$

as the difference of the endpoints. With this convention (3.3) can be written as

$$(3.7) \quad \kappa_k(F_T(u_0)) = (k-1)! \sum_{H \in \mathbb{T}_k} \sum_{\mathbf{x} \in D_H(u_0)} (-1)^{|B_H|-1} f_H(x_1, \dots, x_k) \prod_{j=1}^k \mu_\lambda(x_j).$$

As we already mentioned, the proof of Theorem 3.2 is postponed to Sections 6 to 9.

4. LOW HANGING FRUITS:

FLUCTUATIONS OF THE LAST BOX IN THE BOTTOM ROW

Let T be a Poissonized tableau of shape λ and let $u_0 \in (\lambda_2 - 1, \lambda_1)$. There is only one concave corner with the u -coordinate greater than u_0 ; this corner corresponds to the end of the first row of λ . Schensted insertion $T \leftarrow z$ creates a new box in this corner if and only if z is greater or equal to $T_{\lambda_1,1}$, i.e., the last entry in the first row of T . It follows immediately that for this choice of u_0 the value of the cumulative function of T

$$F_T(u_0) = T_{\lambda_1,1}$$

coincides with the last entry in the first row of T .

Thanks to this observation, if T is a uniformly random Poissonized tableau with fixed shape λ , Theorem 3.2 provides some convenient information about the probability distribution of $T_{\lambda_1,1}$. In many concrete cases we may get some interesting asymptotic results. We start with the following example.

Corollary 4.1 (The corner entry of a rectangular tableau). *Let (p_l) and (q_l) be sequences of positive integers such that $(p_l + q_l)$ tends to infinity and the limit*

$$\alpha = \lim_{l \rightarrow \infty} \frac{q_l}{p_l + q_l}$$

exists. We denote by

$$p_l \times q_l = \underbrace{(q_l, \dots, q_l)}_{p_l \text{ times}}$$

the rectangular Young diagram with p_l rows and q_l columns and by $n_l = p_l q_l$ the number of its boxes. Let $T^{(l)}$ be a uniformly random Poissonized tableau

with shape $p_l \times q_l$. Then the probability distribution of the rightmost box in the first row of $T^{(l)}$ (after a shift and scaling)

$$(4.1) \quad Y^{(l)} := \sqrt[4]{n_l} \left(T_{q_l,1}^{(l)} - \frac{q_l}{p_l + q_l} \right) \xrightarrow[l \rightarrow \infty]{\text{dist}} N(0, \sigma_\alpha)$$

converges to the centered Gaussian distribution with the variance

$$\sigma_\alpha^2 = [\alpha(1 - \alpha)]^{\frac{3}{2}}.$$

This result is due to Marchal [Mar16] who used very different methods. Below we present a new proof.

Proof. The diagram $p_l \times q_l$ has two concave corners with the u -coordinates equal to $-p_l$ and q_l . Kerov's transition measure is supported in these two corners; their probabilities are equal to, respectively, $\frac{q_l}{p_l + q_l}$ and $\frac{p_l}{p_l + q_l}$. Let $u_0 \in (-p_l, q_l)$ be between the u -coordinates of these concave corners.

Theorem 3.2 gives the following values for the first two cumulants of the random variable $F_T(u_0)$:

$$(4.2) \quad \mathbb{E} F_T(u_0) = \frac{q_l}{p_l + q_l},$$

$$(4.3) \quad \text{Var } F_T(u_0) = \frac{q_l}{p_l + q_l} \frac{p_l}{p_l + q_l} \frac{1}{p_l + q_l + 1}.$$

Due to the shift and the scaling it follows that the expected value of the random variable $Y^{(l)}$ on the left-hand side of (4.1) is equal to zero while its variance converges to σ_α^2 , as $l \rightarrow \infty$.

Theorem 3.2 implies that

$$\left| \kappa_k(F_T(u_0)) \right| \leq \frac{|\mathbb{T}_k|}{(p_l + q_l + 1)^{k-1}}.$$

It follows that the k -th cumulant of the random variable on the left-hand side of (4.1) is of order

$$\kappa_k(Y^{(l)}) = O\left((p_l + q_l)^{1-\frac{k}{2}}\right);$$

in particular it converges to zero for $k \geq 3$.

So far we proved that the cumulants of $Y^{(l)}$ converge to their counterparts for the normal distribution on the right-hand side of (4.1), so the convergence of distributions in (4.1) holds true in moments. However, since the normal distribution is uniquely determined by its moments, the convergence in moments implies in this case also convergence in the weak topology of probability measures, as claimed. \square

The above method of proof is also applicable to the case when

$$\lambda^{(k)} = (\underbrace{q_{k,1}, \dots, q_{k,1}}_{p_{k,1} \text{ times}}, \underbrace{q_{k,2}, \dots, q_{k,2}}_{p_{k,2} \text{ times}}, \dots, \underbrace{q_{k,i}, \dots, q_{k,i}}_{p_{k,i} \text{ times}})$$

is a *multi-rectangular Young diagram* obtained by stacking a fixed number of rectangles.

It would be interesting to verify if these tools could be used for the case of the random insertion tableau obtained by applying RSK to a finite sequence of i.i.d. random variables with the uniform distribution $U(0, 1)$ in order to reprove the result of Azangulov [Aza20], see also [MMŚ23, Section 1.8] about the convergence of $n(1 - T_{\lambda_1,1})$ to the exponential distribution.

5. THE DOUBLE CUMULATIVE FUNCTION. PROOF OF THEOREM 2.3

5.1. The double cumulative function. Let a Young diagram λ be fixed; let T be a uniformly random Poissonized tableau of shape λ . We consider the *double cumulative function* of λ

$$\mathcal{F}_\lambda: \mathbb{R} \times [0, 1] \rightarrow [0, 1]$$

which is defined as

$$\mathcal{F}_\lambda(u, z) = \mathbb{P}(\text{u-Ins}(T; z) > u) = \mathbb{P}(F_T(u) \leq z).$$

The key motivation to this definition is that for each fixed u_0 the double cumulative function $[0, 1] \ni z \mapsto \mathcal{F}_\lambda(u_0, z)$ is the cumulative distribution function for the random variable $F_T(u_0)$. In particular, the double cumulative function is weakly increasing with respect to the variable z . It has discontinuities along the vertical lines with the values of the variable u equal to the u -coordinates of the concave corners, see Figure 17 for an example corresponding to $\lambda = (3, 1)$. On each (possibly infinite) rectangular segment between such vertical lines the double cumulative function $\mathcal{F}_\lambda(u, z)$ depends only on the second variable (in fact, it is given by a complicated polynomial in z), see Figure 18 for an example.

On the other hand, if we fix the variable $z \in [0, 1]$, the tail function

$$\mathbb{R} \ni u \mapsto 1 - \mathcal{F}_\lambda(u, z)$$

is the cumulative distribution function of the random variable $\text{u-Ins}(T; z)$ which is very convenient in the context of the proof of Theorem 2.3. In fact, the probability distribution of $\text{u-Ins}(T; z)$ can be seen directly from the collection of plots such as the ones from Figure 18, as follows. The unit interval which corresponds to the fixed value of z is divided into a number of intervals. The lengths of these intervals are the probabilities associated to specific concave corners.

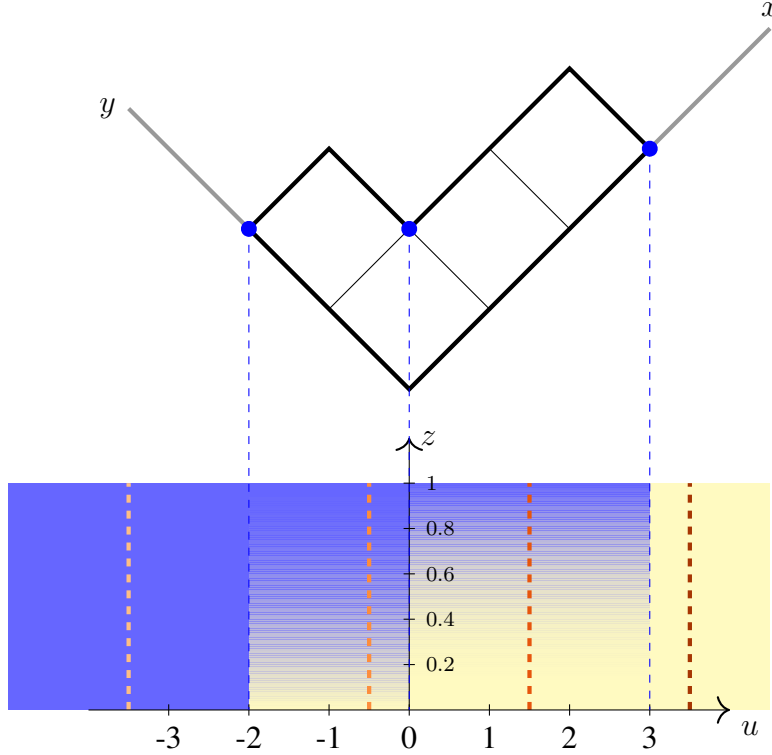


Figure 17. The density plot of the double cumulative function $\mathcal{F}_\lambda(u, z)$ for the Young diagram $\lambda = (3, 1)$. The bright yellow indicates the areas where the insertion function takes values which are close to 0. Dark blue indicates the values which are close to 1. The plots of the double cumulative function along the four vertical dashed lines are shown on Figure 18.

5.2. Examples. The double cumulative function for $\lambda = (3, 1)$ is visualized on Figure 17 as a density plot. The plots of the cumulative function along the four vertical lines are shown on Figure 18.

For a staircase diagram the double cumulative function is visualized on Figure 19 and, for another staircase diagram, on Figure 20.

5.3. Proof of Theorem 2.2.

Lemma 5.1. *Let $(\lambda^{(n)})$ be a sequence of Young diagrams which fulfills the assumptions of Theorem 2.2. Let $u \in \mathbb{R}$ and $z \in [0, 1]$.*

If $z < F_\mu(u^-) = \lim_{v \rightarrow u^-} F_\mu(v)$ then

$$\mathcal{F}_{\lambda^{(n)}}(\sqrt{n} u, z) \xrightarrow[n \rightarrow \infty]{P} 0.$$

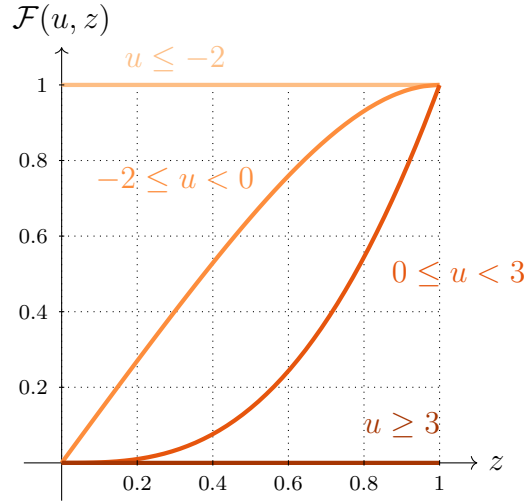


Figure 18. Continuation of the example from Figure 17. Plots of the double cumulative function $z \mapsto \mathcal{F}_\lambda(u, z)$ (viewed as a function of the variable z) with $\lambda = (3, 1)$ for various choices of u .

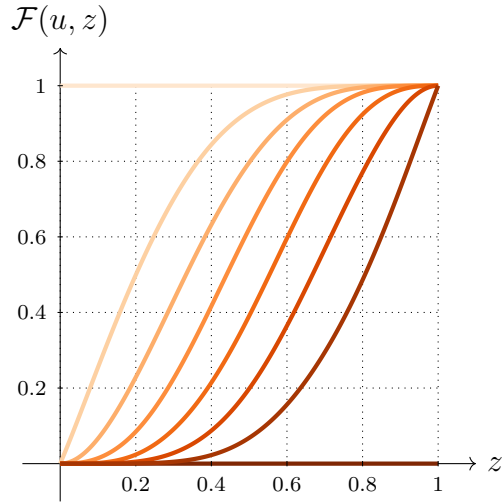


Figure 19. An analogue of Figure 18 for the staircase diagram $\lambda = (6, 5, 4, 3, 2, 1)$. This diagram has 7 concave corners; their u -coordinates divide the real line into 8 finite or infinite intervals. The bright top curve (constantly equal to 1) corresponds to the leftmost (infinite) interval; the dark bottom curve (constantly equal to 0) corresponds to the rightmost (infinite) interval.

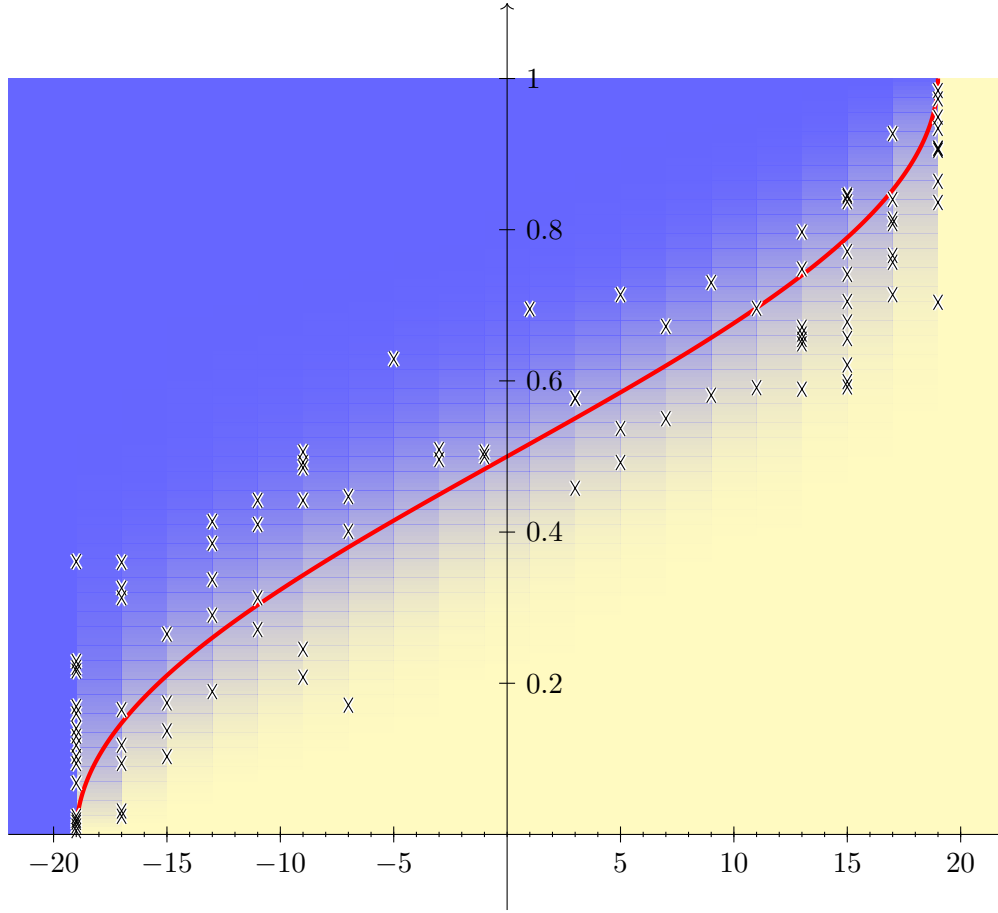


Figure 20. An analogue of Figure 17 for the staircase diagram $\lambda = (19, 18, \dots, 1)$. The crosses show points $(u\text{-Ins}(T; z), z)$ for random points z sampled with the uniform distribution $U(0, 1)$ and T sampled independently random Poissonized tableau with the shape λ . The thick red line is the cumulative distribution function of the (dilated) arcsine law which is the limit measure of the transition measures of large staircase tableaux.

If $z > F_\mu(u)$ then

$$\mathcal{F}_{\lambda^{(n)}}(\sqrt{n} u, z) \xrightarrow[n \rightarrow \infty]{P} 1.$$

This result is illustrated on Figure 20, where the transition region which separates the bright area and the dark area is roughly the plot of the cumulative distribution function of the arc-sine distribution (the thick red line).

Proof. We start with the first part. There exists $u' < u$ such that $F_\mu(u') > z$. Additionally we may assume that u' is a point of continuity of F_μ .

The probability of the event $K_{\lambda^{(n)}}(u') \leq z$ converges to zero; for our purposes of proving convergence in probability we can ignore this event.

Let us *condition* for a moment over the event that the diagram $\lambda^{(n)}$ is fixed and such that $K_{\lambda^{(n)}}(u') > z$. As usual, by $T^{(n)}$ we denote the uniformly random Poissonized tableau with shape $\lambda^{(n)}$. From the explicit formula (3.5) it follows that the *conditional* variance fulfills

$$\int_{\sqrt{n} u'}^{\sqrt{n} u} \text{Var } F_{T^{(n)}}(v) dv \leq 1;$$

it follows that there exists $u_n \in [u', u]$ with the property that

$$\text{Var } F_{T^{(n)}}(u_n) \leq \frac{1}{(u - u')\sqrt{n}}.$$

From the assumption that

$$\mathbb{E} F_{T^{(n)}}(u_n) = K_{\lambda^{(n)}}(u_n) \geq K_{\lambda^{(n)}}(u') > z$$

it follows that the Bienaymé–Chebyshev inequality is applicable and

$$0 \leq \mathcal{F}_{\lambda^{(n)}}(u, z) \leq \mathcal{F}_{\lambda^{(n)}}(u_n, z) = \mathbb{P}(F_{T^{(n)}} \leq z) \leq \frac{\text{Var } F_{T^{(n)}}(u_n)}{(\mathbb{E} F_{T^{(n)}}(u_n) - z)^2} \leq \frac{1}{(u - u')\sqrt{n} (K_{\lambda^{(n)}}(u') - z)^2}$$

Since the right-hand side converges to zero, this completes the proof of the first part of the claim.

We can forget now about the conditioning; we proved that

$$0 \leq \mathcal{F}_{\lambda^{(n)}}(u, z) \leq \begin{cases} \frac{1}{(u - u')\sqrt{n} (K_{\lambda^{(n)}}(u') - z)^2} & \text{if } K_{\lambda^{(n)}}(u') > z \\ 1 & \text{otherwise.} \end{cases}$$

Since the random variable on the right-hand side converges in probability to zero, this completes the proof.

The second part follows in a fully analogous way. \square

Proof of Theorem 2.2. It is a straightforward application of Lemma 5.1. \square

5.4. Proof of Theorem 2.3.

Lemma 5.2. *Let G be a bipartite tree (with each vertex colored black or white, and each edge connecting the vertices of opposite colors) with $k \geq 1$ vertices. We assume that G is an oriented graph (with each edge oriented from the black endpoint to the white endpoint) and weighted (with the weight of each edge greater or equal to 1).*

Let μ be a discrete probability measure on \mathbb{R} , and let $u_0 \in \mathbb{R}$.
Then

$$S(G) := \sum_{\mathbf{x}} \frac{\prod_{v \in V_G} \mu(\mathbf{x}(v))}{\prod_{e=(i,j) \in E_G} (\mathbf{x}(j) - \mathbf{x}(i) + w(e))} \leq \left[\mathbf{G}_{\mu}^+(u_0) \right]^{n-1},$$

where the sum on the left-hand side runs over the u_0 -decorations of the vertices of G .

Proof. We use induction over the number of the vertices.

For $n = 1$ there is nothing to prove.

For $n \geq 2$ let w be a leaf of G and let G' be the tree G after removal of the vertex w and the adjacent edge. By a straightforward bound on the factor which corresponds to the unique edge adjacent to G it follows that

$$S(G) \leq S(G') \mathbf{G}_{\mu}^+(u_0)$$

and the inductive step follows immediately. \square

Proof of Theorem 2.3. We start with the special case when each of the diagrams $\lambda^{(n)}$ is deterministic.

Let us fix $c \in \mathbb{R}$; we denote

$$U_n = \sqrt{n} u_0 + \sqrt[4]{n} c$$

and we consider the random variable

$$X_n = \frac{\sqrt[4]{n}}{\sqrt{\mathcal{E}}} \left[F_{T^{(n)}}(U_n) - \left(z + \frac{fc}{\sqrt[4]{n}} \right) \right].$$

By simple algebra and (3.1) it follows that the tail probability for the random variable in (2.9) is given by

$$(5.1) \quad \mathbb{P} \left(\frac{\text{u-Ins}(T^{(n)}; z) - \sqrt{n} u_0}{\sqrt[4]{n}} \geq c \right) = \mathcal{F}_{\lambda^{(n)}}(U_n, z) = \\ \mathbb{P}(\text{u-Ins}(T^{(n)}; z) \geq U_n) = \mathbb{P}(F_{T^{(n)}}(U_n) \leq z) = \\ \mathbb{P} \left(X_n \leq -\frac{fc}{\sqrt{\mathcal{E}}} \right).$$

We will use Theorem 3.2 in order to calculate the cumulants of the random variable X_n which appears on the right-hand side. The first cumulant $\mathbb{E}X_n$ tends to zero by the assumption (a). The second cumulant $\text{Var } X_n$ converges to 1 by the assumption (b). For $k \geq 3$ the absolute value of the corresponding cumulant can be bounded thanks to Lemma 5.2 and the assumption (c)

$$(5.2) \quad \kappa_k(X_n) = o \left(n^{\frac{k}{4} - \alpha(k-1)} \right)$$

which tends to zero if $\alpha > \frac{3}{8}$. In this way we proved that the sequence (X_n) converges in moments to the standard normal distribution $N(0, 1)$; since the normal distribution is uniquely determined by its moments, the latter convergence holds true also in the weak topology of probability measures. This convergence is illustrated on Figure 19, where each of the plots can be approximated by the cumulative distribution function of some Gaussian measure.

As a consequence we have the convergence of the right-hand side of (5.1) thus

$$(5.3) \quad \mathbb{P} \left(\frac{\text{u-Ins}(T^{(n)}; z) - \sqrt{n} u_0}{\sqrt[4]{n}} \geq c \right) \xrightarrow{n \rightarrow \infty} \Phi \left(-\frac{fc}{\sqrt{\mathcal{E}}} \right) = 1 - \Phi \left(\frac{fc}{\sqrt{\mathcal{E}}} \right),$$

where

$$\Phi(x) = \frac{1}{\sqrt{2\pi}} \int_{-\infty}^x e^{-\frac{t^2}{2}} dt$$

denotes the cumulative distribution function of the standard normal distribution. Equation (5.3) gives the asymptotics of the tail probabilities for the random variables from the statement of the theorem which concludes the proof in the case when the Young diagrams $\lambda^{(n)}$ are all deterministic.

We will revisit the above proof in the general case when the Young diagrams $\lambda^{(n)}$ are random.

Firstly, the probabilities which appear in (5.1) and (5.3) should be understood as *conditional probabilities*, under the condition that the Young diagram $\lambda^{(n)}$ is fixed; such conditional probabilities are random variables, functions of $\lambda^{(n)}$. In particular, the convergence in (5.3) should be interpreted now as *convergence in probability*; we will justify its validity below.

Fix $\epsilon > 0$. By a fairly standard argument [RS15, Section 4.10] there exists a $\delta > 0$ and an integer $A > 0$ with the property that if m is a probability measure on \mathbb{R} such that its moments (up to order A) are δ -close to the moments of the standard Gaussian measure then

$$|F_\mu(x) - F_{\text{SC}}(x)| < \epsilon$$

holds true for $x = -\frac{fc}{\sqrt{\mathcal{E}}}$. This shows that if the *conditional* moments of X_n (given the value of $\lambda^{(n)}$) converge *in probability* towards the corresponding moments of the standard Gaussian measure then the convergence in (5.3) holds true in probability as well.

We are interested in the *unconditional* probability

$$\mathbb{P} \left(\frac{\text{u-Ins}(T^{(n)}; z) - \sqrt{n} u_0}{\sqrt[4]{n}} \geq c \right)$$

which is equal to the expected value of the left-hand side of (5.3); fortunately applying the expected value to (5.3) can be justified easily. \square

Remark 5.3. It seems that the condition (c) in Theorem 2.3 can be weakened, and it is enough to assume that $\alpha > \frac{1}{4}$. In this case the cumulant $\kappa_k(X_n)$ in (5.2) tends to zero if k is big enough. We first choose a sequence (C_n) with $C_n \geq 1$ such that there is a subsequence of the rescaled sequence $\frac{1}{C_n}X_n$ which converges in moments and weakly to some limit which is not supported in $\{0\}$. The limit measure has only finitely many non-zero cumulants so by Marcinkiewicz theorem it is a Gaussian measure. This shows that in fact we can choose $C_n = 1$. The above reasoning shows that from each subsequence of (X_n) one can choose a subsequence converging to the standard Gaussian measure; it follows that (X_n) converges as well. We did not pursue to make this sketch rigorous.

6. ANTI-PIERI GROWTH PROCESS

We slowly prepare for the proof of Theorem 3.2. The proof will culminate in Section 9.

The aforementioned results of Romik and the second named author were proved using the *anti-Pieri growth process* [RS15, Section 4.1]. It should come as no surprise that we also will use this growth process.

6.1. Proof of Lemma 2.1.

Proof of Lemma 2.1. In the following we consider the unit cube

$$[0, 1]^n = \{(w_1, \dots, w_n) : w_1, \dots, w_n \in [0, 1]\}$$

(equipped with the Lebesgue measure) with all hyperplanes $w_i - w_j = 0$ (over $1 \leq i < j \leq n$) removed. Since the removed hyperplanes have Lebesgue measure zero, this removal is irrelevant from the viewpoint of the measure theory. The hyperplanes divide the cube into $n!$ isometric simplices, each with the volume $\frac{1}{n!}$. The simplices are in a bijective correspondence with permutations in \mathfrak{S}_n ; each simplex \mathcal{S}_σ consists of the vectors with a prescribed linear order between the coordinates.

For a given Young diagram λ we denote by \mathcal{T}^λ the set of Poissonized tableaux of shape λ , equipped with the Lebesgue measure. For simplicity we remove from this set all tableaux which have repeated entries; again this removal is irrelevant from the viewpoint of the measure theory.

With these notations, the Robinson–Schensted correspondence is a bijection between the aforementioned cube $[0, 1]^n$ and the disjoint sum

$$(6.1) \quad \bigsqcup_{\lambda \vdash n} \mathcal{T}^\lambda \times f^\lambda,$$

where f^λ denotes the set of standard Young tableaux of shape λ . The second component of this correspondence, the map Q , restricted to the simplex \mathcal{S}_σ is constant, equal to the recording tableau $Q(\sigma)$. On the other hand, the first component of this correspondence, the map P , restricted to \mathcal{S}_σ acts by arranging the entries of (w_1, \dots, w_n) to the boxes of the diagram $\text{RSK}(\sigma)$. It follows that the Robinson–Schensted correspondence is a piecewise isometry, hence it is a measure-preserving map if we equip f^λ with the counting measure and each summand in (6.1) with the product measure.

Conditioning over the event $\text{RSK}(w) = \lambda$ corresponds therefore to considering the uniform measure (or, equivalently, the product measure multiplied by the scalar factor $\frac{n!}{(f^\lambda)^2}$) on a specific summand of (6.1), namely

$$\mathcal{T}^\lambda \times f^\lambda$$

which completes the proof. \square

6.2. Anti-Pieri growth process. We will use the following notation which is intended as an analogue of the falling factorial

$$\mathbf{G}_\lambda^k(x) = \begin{cases} \underbrace{\mathbf{G}_\lambda(x) \mathbf{G}_\lambda(x-1) \cdots \mathbf{G}_\lambda(x-k+1)}_{k \text{ factors}} & \text{if } k \geq 1, \\ 1 & \text{if } k = 0 \end{cases}$$

for an integer $k \geq 0$.

Lemma 6.1. *Let λ be a fixed Young diagram with n boxes and $k \geq 1$ be an integer.*

Let

$$\lambda = \xi_n \nearrow \xi_{n+1} \nearrow \cdots \nearrow \xi_{n+k}$$

be given by the Plancherel growth process starting at λ and let $\mathbf{U} = (U_1, \dots, U_k)$ be the sequence of the u -coordinates of the boxes added in each step, i.e.,

$$U_i = u(\xi_{n+i} \setminus \xi_{n+i-1})$$

for $i \in \{1, \dots, k\}$.

(a) *Let T be a random Poissonized tableau of shape λ . Then for any $u_0 \in \mathbb{R}$ the moment of the random variable $F_T(u_0)$ fulfills*

$$\begin{aligned} m_k(F_T(u_0)) &= \mathbb{E} \left[(F_T(u_0))^k \right] \\ &= k! \mathbb{P}(u_0 \geq U_1 > \cdots > U_k). \end{aligned}$$

(b) *if $U_1 > \cdots > U_k$ then the tuple $\mathbf{U} = (U_1, \dots, U_k)$ can be uniquely written in the form*

$$\mathbf{x}^{\mathbf{a}} = \left(\underbrace{x_1, x_1 - 1, \dots, x_1 - a_1 + 1}_{a_1 \text{ times}}, \dots, \underbrace{x_\ell, x_\ell - 1, \dots, x_\ell - a_\ell + 1}_{a_\ell \text{ times}} \right)$$

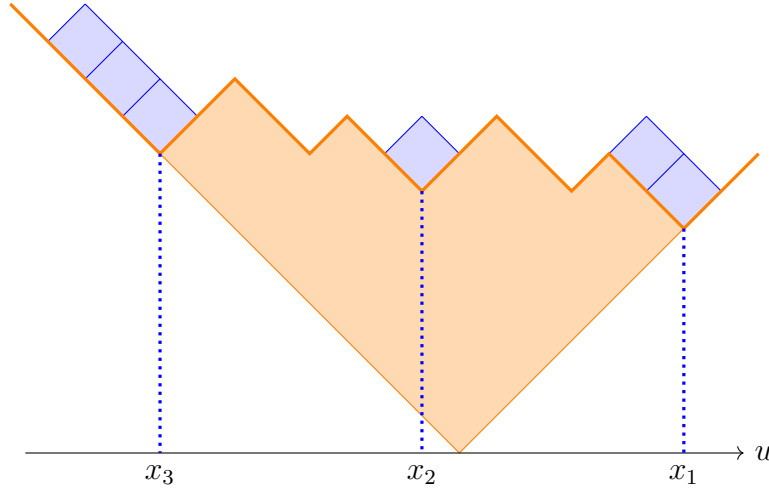


Figure 21. Example of the growth of a Young diagram considered in Lemma 6.1. The orange area is the original Young diagram λ , the blue boxes are being added in successive steps, from right to left. The quantities from Lemma 6.1(b) are as follows: $a_1 = 2$, $a_2 = 1$, $a_3 = 3$.

with $\mathbf{x} = (x_1, \dots, x_\ell)$ and $\mathbf{a} = (a_1, \dots, a_\ell)$, where $x_1 > \dots > x_\ell$ are u -coordinates of some concave corners of λ and $a_1, \dots, a_\ell \geq 1$ are integers such that $a_1 + \dots + a_\ell = k$, see Figure 21.

- (c) Let x_1, \dots, x_ℓ be the u -coordinates of some concave corners of λ . Let $a_1, \dots, a_\ell \geq 1$ be integers such that $a_1 + \dots + a_\ell = k$. We assume that the following condition holds true:

(X) for each $i \in \{1, \dots, \ell\}$ the set

$$\{x_i - 1, x_i - 2, \dots, x_i - a_i + 1\}$$

and the set of u -coordinates of the concave corners of λ are disjoint.

Then

$$(6.2) \quad \mathbb{P}[\mathbf{U} = \mathbf{x}^{\mathbf{a}}] = \Theta(x_1, \dots, x_\ell) \prod_{1 \leq i \leq \ell} \frac{(-1)^{a_i-1}}{a_i} \mu_\lambda(x_i) \mathbf{G}_\lambda^{a_i-1}(x_i - 1),$$

where

$$(6.3) \quad \Theta(x_1, \dots, x_\ell) = \prod_{1 \leq i < j \leq \ell} \frac{(x_i - x_j)(x_i - x_j - a_i + a_j)}{(x_i - x_j + a_j)(x_i - x_j - a_i)}.$$

Note that the assumption (X) guarantees that on the right-hand side of (6.2) we do not evaluate the Cauchy transform \mathbf{G}_λ or the function Θ in a singularity.

Proof. Proof of part (a). Our general strategy is to create a coupling and to create on a single probability space both a uniformly random Poissonized tableau with shape λ , as well as a Plancherel growth process starting in λ . A small additional difficulty is that our model will require some conditioning.

Let w_1, \dots, w_{n+k} be a sequence of independent random variables with the uniform distribution $U(0, 1)$ and let $\Xi_i = \text{RSK}(w_1, \dots, w_i)$; then

$$\Xi_0 \nearrow \dots \nearrow \Xi_{n+k}$$

is the Plancherel growth process. For $i \in \{1, \dots, k\}$ we denote by $\mathcal{U}_i = u(\Xi_{n+i} \setminus \Xi_{n+i-1})$ the u -coordinate of the place where the growth occurs.

Clearly, the probability distribution of the Plancherel growth process $(\xi_n, \dots, \xi_{n+k})$ starting at $\xi_n = \lambda$ coincides with the *conditional* probability distribution of its counterpart $(\Xi_n, \dots, \Xi_{n+k})$, under the condition that $\Xi_n = \lambda$. By Lemma 2.1, the probability distribution of the random Poissonized tableau T from the statement of the lemma coincides with the *conditional* probability distribution of the insertion tableau $\mathcal{T} := P(w_1, \dots, w_n)$, under the condition $\Xi_n = \lambda$.

These observations imply that it is enough to prove equality between the conditional expectations

(6.4)

$$\mathbb{E} \left[(F_{\mathcal{T}}(u_0))^k \mid \sigma(\Xi_n) \right] = k! \mathbb{E} \left[\mathbb{1}(u_0 \geq \mathcal{U}_1 > \dots > \mathcal{U}_k) \mid \sigma(\Xi_n) \right],$$

where $\sigma(\Xi_n)$ denotes the σ -algebra generated by the random Young diagram Ξ_n , and $\mathbb{1}\{A\}$ denotes the indicator random variable which takes the value 1 if the condition A holds true, and 0 otherwise.

For a moment let us fix the values in the prefix x_1, \dots, x_n ; the conditional probability

(6.5)

$$\begin{aligned} & \mathbb{P} \left[F_{\mathcal{T}}(u_0) > w_{n+1} > \dots > w_{n+k} \mid \sigma(x_1, \dots, x_n) \right] \\ &= \mathbb{E} \left[\mathbb{1} \{ F_{\mathcal{T}}(u_0) > w_{n+1} > \dots > w_{n+k} \} \mid \sigma(x_1, \dots, x_n) \right] \\ &= \text{vol} \left\{ (x_{n+1}, \dots, x_{n+k}) \in [0, 1]^k : F_{\mathcal{T}}(u_0) > w_{n+1} > \dots > w_{n+k} \right\} \\ &= \frac{1}{k!} [F_{\mathcal{T}}(u_0)]^k \end{aligned}$$

is then directly related to the value of the random variable $F_{\mathcal{T}}(u_0)$.

The event which appears on the left hand side of (6.5) can be alternatively reformulated in the language of the Young diagrams $\Xi_n \nearrow \dots \nearrow \Xi_{n+k}$ as follows:

$$(6.6) \quad \{F_T(u_0) > w_{n+1} > \dots > w_{n+k}\} = \{u_0 \geq \mathcal{U}_1 > \dots > \mathcal{U}_k\}.$$

Indeed, the equivalence

$$F_T(u_0) > w_{n+1} \iff u_0 \geq \mathcal{U}_1$$

is a consequence of the definition of $F_T(u_0)$ while each of the equivalences

$$w_{n+i} > w_{n+i+1} \iff \mathcal{U}_i > \mathcal{U}_{i+1}$$

is the content of the Row Bumping Lemma [Ful97, page 9]. Thus, by taking the appropriate conditional expectation of both sides of (6.5), the desired equality (6.4) follows immediately.

The part (b) is obvious.

Proof of part (c). We start with the case when the probability on the left-hand side of (6.2) is non-zero. For an illustration see Figure 21. For integers $j \in \{1, \dots, \ell\}$ and $m \in \{0, \dots, a_j\}$ we define the Young diagram $\lambda^{[j,m]}$ as the diagram λ with additional boxes, the u -coordinates of which form the following multiset

$$\underbrace{x_1, x_1 - 1, \dots, x_1 - a_1 + 1}_{a_1 \text{ elements}}, \dots, \underbrace{x_{j-1}, x_{j-1} - 1, \dots, x_{j-1} - a_{j-1} + 1}_{a_{j-1} \text{ elements}}, \\ \underbrace{x_j, x_j - 1, \dots, x_j - m + 1}_m \text{ elements}.$$

Note that $\lambda^{[j,a_j]} = \lambda^{[j+1,0]}$. With this notation, the event $\mathbf{U} = \mathbf{x}^{\mathbf{a}}$ holds if and only if the sequence $(\xi_n, \dots, \xi_{n+k})$ is equal to

$$(6.7) \quad \left(\underbrace{\lambda^{[1,0]}, \dots, \lambda^{[1,a_1]}}_{a_1 + 1 \text{ elements}}, \underbrace{\lambda^{[2,1]}, \dots, \lambda^{[2,a_2]}}_{a_2 \text{ elements}}, \dots, \underbrace{\lambda^{[\ell,1]}, \dots, \lambda^{[\ell,a_\ell]}}_{a_\ell \text{ elements}} \right) = \\ \left(\underbrace{\lambda^{[1,0]}, \dots, \lambda^{[1,a_1-1]}}_{a_1 \text{ elements}}, \dots, \underbrace{\lambda^{[\ell-1,0]}, \dots, \lambda^{[\ell-1,a_{\ell-1}-1]}}_{a_{\ell-1} \text{ elements}}, \underbrace{\lambda^{[\ell,0]}, \dots, \lambda^{[\ell,a_\ell]}}_{a_\ell + 1 \text{ elements}} \right)$$

It follows that we need to calculate the probability that a Plancherel growth process starting in $\lambda = \lambda^{[1,0]}$ in the first k steps will traverse the diagrams (6.7). Since it is a Markov process, we need to calculate the probability of each transition separately and then take the product. We will consider separately the transitions in which a new box is created in one of the concave corners of the original diagram λ and the remaining ones.

Transition from $\lambda^{[j,0]}$ to $\lambda^{[j,1]}$. The diagram $\lambda^{[j,0]}$ can be obtained from λ by adding $j - 1$ rectangles, see Figure 21. The i -th rectangle (with $i \in \{1, \dots, j - 1\}$) has the following four vertices:

- the bottom and the top vertex, with the u -coordinates equal to, respectively, x_i and $x_i - a_i + 1$; each of these two vertices is either responsible for removal of a concave corner of λ or for creation of a new convex corner; both of these operations correspond to adding an additional zero to the Cauchy transform, and
- the right and the left vertex, with the u -coordinates equal to, respectively, $x_i + 1$ and $x_i - a_i$; each of these two vertices is either responsible for removal of a convex corner of λ or for creation of a new concave corner; both of these operations correspond to an additional an additional pole to the Cauchy transform.

It follows that

$$\mathbf{G}_{\lambda^{[j,0]}}(z) = \mathbf{G}_{\lambda}(z) \prod_{i \in \{1, \dots, j-1\}} \frac{(z - x_i)(z - x_i + a_i - 1)}{(z - x_i - 1)(z - x_i + a_i)}.$$

Thus the transition probability from the diagram $\lambda^{[j,0]}$ to $\lambda^{[j,1]}$ is equal to the residue

$$(6.8) \quad \text{Res}_{x_j} \mathbf{G}_{\lambda^{[j,0]}}(z) = (\text{Res}_{x_j} \mathbf{G}_{\lambda}(z)) \prod_{i \in \{1, \dots, j-1\}} \frac{(x_j - x_i)(x_j - x_i + a_i - 1)}{(x_j - x_i - 1)(x_j - x_i + a_i)} = \mu_{\lambda}(x_j) \prod_{i \in \{1, \dots, j-1\}} \frac{(x_j - x_i)(x_j - x_i + a_i - 1)}{(x_j - x_i - 1)(x_j - x_i + a_i)}.$$

Transition from $\lambda^{[j,m]}$ to $\lambda^{[j,m+1]}$ for $m > 0$. The diagram $\lambda^{[j,m]}$ can be obtained from λ by adding j rectangles thus

$$\mathbf{G}_{\lambda^{[j,m]}}(z) = \mathbf{G}_{\lambda}(z) \prod_{i \in \{1, \dots, j-1\}} \frac{(z - x_i)(z - x_i + a_i - 1)}{(z - x_i - 1)(z - x_i + a_i)} \times \frac{(z - x_j)(z - x_j + m - 1)}{(z - x_j - 1)(z - x_j + m)}.$$

It follows that the transition probability from the diagram $\lambda^{[j,m]}$ to $\lambda^{[j,m+1]}$ is equal to the residue

$$(6.9) \quad \text{Res}_{x_j-m} \mathbf{G}_{\lambda^{[j,0]}}(z) = \mathbf{G}_{\lambda}(x_j - m) \times \prod_{i \in \{1, \dots, j-1\}} \frac{(x_j - m - x_i)(x_j - m - x_i + a_i - 1)}{(x_j - m - x_i - 1)(x_j - m - x_i + a_i)} \cdot \frac{(-1)m}{m+1}.$$

The product. We consider the probability (6.8) multiplied with the product of (6.9) over all choices of $m \in \{1, \dots, a_j - 1\}$. Due to some telescopic cancellations this whole product is equal to

$$\mu_{\lambda}(x_j) \mathbf{G}_{\lambda}^{a_j-1}(-1)^{a_j-1} \frac{1}{a_j} \prod_{i \in \{1, \dots, j-1\}} \frac{x_j - x_i}{x_j - x_i - a_j} \cdot \frac{x_j - x_i + a_i - a_j}{x_j - x_i + a_i}.$$

By taking the product over all choices of $j \in \{1, \dots, \ell\}$ we recover the right-hand side of (6.2), as required.

We consider now the case when the probability on the left-hand side of (6.2) is equal to zero. This means that at least one of the diagrams in the sequence (6.7) is not well-defined. Let $\lambda^{[j,m]}$ with $j \in \{1, \dots, \ell\}$ and $m \in \{1, \dots, a_j\}$ be the first entry of this sequence which is not well-defined. This may happen only if $x_j - m + 1$ is the u -coordinate of a convex corner of λ hence $\mathbf{G}_{\lambda}(x_j - m + 1) = 0$ and $m \geq 2$. As a consequence, one of the factors on the right-hand side of (6.2) is equal to zero, as required. \square

7. DECOMPOSITION INTO SIMPLE FRACTIONS

In this section we will decompose the product Θ defined in (6.3) into a sum of simple fractions.

A *spine graph* with $\ell \geq 1$ vertices is defined as a connected directed graph F such that the set of its edges consists of $\ell - 1$ elements and is of the form

$$E_F = \{(v_1, v_2), \dots, (v_{\ell-1}, v_{\ell})\}.$$

Note that the vertices v_1, \dots, v_{ℓ} are all different; otherwise, the graph would not be connected. We denote the set of all spine graphs with the vertex set $V = \{1, \dots, \ell\}$ by S_{ℓ} ; obviously $|S_{\ell}| = \ell!$. An example of a spine graph is shown in Figure 22.

A *multi-spine graph* is defined as any directed graph such that each component is a spine graph. In other words, a multi-spine graph is a forest of spine graphs. We denote the set of all multi-spine graphs with the vertex set $V = \{1, \dots, \ell\}$ by MS_{ℓ} . An example of a multi-spine graph is shown in Figure 23.



Figure 22. An example of a spine graph with 6 vertices.

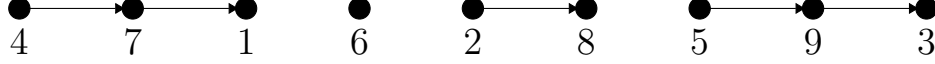


Figure 23. An example of a multi-spine graph with 9 vertices and 4 connected components.

Lemma 7.1. *Let (a_1, \dots, a_ℓ) be a sequence of numbers which has the property that the sum of the entries of any non-empty subsequence is non-zero (this condition holds, for example, if $a_1, \dots, a_\ell > 0$ are all positive).*

Then the element $\Theta \in \mathbb{R}(x_1, \dots, x_\ell)$ of the field of rational functions defined in (6.3) can be written as the sum

$$(7.1) \quad \Theta(x_1, \dots, x_\ell) = \sum_{F \in \text{MS}_\ell} \frac{\beta_F}{\prod_{(i,j) \in E_F} (x_j - x_i + a_i)}.$$

Above, for any graph $F \in \text{MS}_\ell$, the constant β_F is defined as

$$(7.2) \quad \beta_F = (-1)^{|V_F|} \frac{\prod_{j=1}^{\ell} a_j}{\prod_{F'} \left[(-1) \cdot \sum_{i \in V_{F'}} a_i \right]},$$

where the product over F' runs over all connected components of the graph F .

Proof. To simplify the notation, we put

$$z_j = x_j - a_j$$

for each index $j \in \{1, \dots, \ell\}$.

Let

$$A = \left[\frac{1}{x_i - z_j} \right]_{1 \leq i, j \leq \ell}$$

be the Cauchy matrix [Sch59]. Its determinant, called the *Cauchy determinant*, is given by the following product formula [Sch59]

$$\det A = \frac{\prod_{1 \leq i < j \leq \ell} (x_i - x_j)(z_j - z_i)}{\prod_{1 \leq i, j \leq \ell} (x_j - z_i)}.$$

The denominator of Θ differs from its counterpart in the Cauchy determinant only by the missing diagonal factors $x_j - z_i$ for $i = j$. Thus

$$\Theta = \left(\prod_{j=1}^{\ell} (x_j - z_j) \right) \det A = \left(\prod_{j=1}^{\ell} a_j \right) \det A.$$

Using the definition of the determinant we express Θ as a sum over permutations

$$\Theta = \left(\prod_{j=1}^{\ell} a_j \right) \sum_{\sigma \in \mathfrak{S}_k} \frac{(-1)^{\ell-c(\sigma)}}{\prod_{i=1}^{\ell} (x_{\sigma(i)} - z_i)},$$

where $c(\sigma)$ denotes the number of cycles of the permutation σ . We can treat each permutation $\sigma \in \mathfrak{S}_n$ as a directed weighted graph with the vertex set $V_{\sigma} = \{1, \dots, \ell\}$ and with the edge set

$$E_{\sigma} = \left\{ (1, \sigma(1)), \dots, (\ell, \sigma(\ell)) \right\}.$$

We define the weight of an edge $e = (i, \sigma(i))$ as $w(e) = a_i$. Therefore

$$\Theta = \left(\prod_{j=1}^{\ell} a_j \right) \sum_{\sigma \in \mathfrak{S}_k} (-1)^{\ell-c(\sigma)} f_{\sigma} = (-1)^{\ell} \left(\prod_{j=1}^{\ell} a_j \right) \sum_{\sigma \in \mathfrak{S}_k} \prod_{\sigma'} (-f_{\sigma'}),$$

where σ' runs over the connected components of the directed graph σ ; note that each such connected component corresponds to a cycle of the permutation σ .

Let σ' be a connected component of the directed graph σ . Using the identity

$$\sum_{i \in V_{\sigma'}} a_i = \sum_{j \in V_{\sigma'}} x_j - \sum_{i \in V_{\sigma'}} z_i = \sum_{(i,j) \in E_{\sigma'}} (x_j - z_i)$$

we obtain

$$(7.4) \quad f_{\sigma'} \sum_{i \in V_{\sigma'}} a_i = f_{\sigma'} \sum_{(i,j) \in E_{\sigma'}} (x_j - z_i) = \sum_{F'} f_{F'},$$

where F' runs over all spine graphs obtained from the cycle σ' by removing exactly one edge.

Equation (7.4) can be written as

$$f_{\sigma'} = \frac{1}{\sum_{i \in V_{\sigma'}} a_i} \sum_{F'} f_{F'};$$

we apply this identity to each cycle σ' of the permutation $\sigma \in \mathfrak{S}_k$ on the right-hand side of (7.3). Note that the above equality holds true also in the

special case when the cycle σ' is a fix-point; in this case we remove the loop from the directed graph σ' , and the unique resulting graph F' has one isolated vertex and no edges.

If we remove one edge from each cycle of every permutation in all possible ways, we obtain each multi-spine graph on the vertex set $\{1, \dots, \ell\}$ exactly once. In this way we proved that

$$\Theta = (-1)^\ell \left(\prod_{j=1}^{\ell} a_j \right) \sum_{F \in \text{MS}_\ell} \prod_{F'} \frac{-f_{F'}}{\sum_{i \in V_{F'}} a_i}$$

where F' runs over the connected components of the graph F , as required. \square

8. THE MOMENTS OF THE CUMULATIVE FUNCTION

8.1. The first formula for the moments. A *composition* of a natural number k is an expression of k as an ordered sum of positive integers $k = a_1 + \dots + a_\ell$. The set of all compositions of k will be denoted by Comp_k . For a given composition $\mathbf{a} = (a_1, \dots, a_\ell) \in \text{Comp}_k$ we denote the number of its parts by $\ell = \ell(\mathbf{a})$.

Using Lemma 6.1 we obtain

$$\begin{aligned} (8.1) \quad m_k(F_T(u_0)) &= k! \sum_{\mathbf{a} \in \text{Comp}_k} \sum_{\mathbf{x}} \mathbb{P}[\mathbf{U} = \mathbf{x}^{\mathbf{a}}] \\ &= k! \sum_{\mathbf{a} \in \text{Comp}_k} \sum_{\mathbf{x}} \Theta(x_1, \dots, x_\ell) \prod_{i=1}^{\ell} \frac{(-1)^{a_i-1}}{a_i} \mu_\lambda(x_i) \mathbf{G}_\lambda^{\frac{a_i-1}{\lambda}}(x_i - 1), \end{aligned}$$

where in each expression the second sum runs over $\mathbf{x} = (x_1, \dots, x_\ell) \in \mathbb{X}$ such that

$$(8.2) \quad u_0 \geq x_1 > x_2 > \dots > x_\ell$$

and such that the condition (X) from Lemma 6.1 is satisfied.

The aforementioned condition (X) turns out to be quite cumbersome in applications. For this reason our strategy is to obtain an analogue of the above formula (8.1) which would involve summation over *all* $x_1, \dots, x_\ell \in \mathbb{X}$ which fulfill (8.2), i.e., to remove the requirement (X). Regretfully, without this additional condition it might happen that one of the factors in the falling product $\mathbf{G}_\lambda^{\frac{a_i-1}{\lambda}}(x_i - 1)$ is evaluated in a singularity; thus the right-hand side of (8.1) might involve division by zero.

In order to avoid this difficulty instead of Young diagrams we will consider a more general class of objects, namely *interlacing sequences*, for

which such a division by zero can be easily avoided. The formulas for the Young diagram λ can be then obtained by an appropriate limit.

8.2. Interlacing sequences. The following notations are based on the work of Kerov [Ker93]. We say that

$$(8.3) \quad \Lambda = (\mathbb{x}_0, \dots, \mathbb{x}_\mathbb{L}; \mathbb{y}_1, \dots, \mathbb{y}_\mathbb{L})$$

is an *interlacing sequence* if its entries are real numbers such that

$$\mathbb{x}_0 < \mathbb{y}_1 < \mathbb{x}_1 < \dots < \mathbb{y}_\mathbb{L} < \mathbb{x}_\mathbb{L}.$$

Following Figure 9 and Section 2.2, each Young diagram can be regarded as a specific interlacing sequence. Conversely, each interlacing sequence can be visualized as the zig-zag curve analogous to the one from Figure 9; for this reason we will refer to the entries of the sequence $\mathbb{x}_0, \dots, \mathbb{x}_\mathbb{L}$ as *concave corners* and to the entries of the sequence $\mathbb{y}_1, \dots, \mathbb{y}_\mathbb{L}$ as *convex corners*.

The Cauchy transform \mathbf{G}_Λ and the transition measure μ_Λ of an interlacing sequence Λ is defined in an analogous way as their counterparts for Young diagrams in Section 2.2.

8.3. Moments for interlacing sequences. Let an interlacing sequence Λ be fixed. We assume that the set of concave corners is *generic*, i.e., if $i \neq j$ then $\mathbb{x}_i - \mathbb{x}_j$ is *not* an integer. For the set of decoration values $\mathbb{X} := \{\mathbb{x}_0, \dots, \mathbb{x}_\mathbb{L}\}$ we take the concave corners. Let u_0 be a fixed real number. We define the k -th *moment* for the interlacing sequence Λ as

$$(8.4) \quad M_k = M_k(\Lambda, u_0) = k! \sum_{\mathbf{a} \in \mathcal{C}_n} \sum_{\mathbf{x}} \Theta(x_1, \dots, x_\ell) \prod_{i=1}^{\ell} \frac{(-1)^{a_i-1}}{a_i} \mu_\Lambda(x_i) \mathbf{G}_\Lambda^{a_i-1}(x_i - 1),$$

where the sum over \mathbf{x} runs over $x_1, \dots, x_\ell \in \mathbb{X}$ such that (8.2) holds true, and $\ell = \ell(\mathbf{a})$ denotes the length of the composition \mathbf{a} as before. The assumption that the set of concave corners is generic guarantees that the right-hand side is well-defined. One can ask if the quantity $M_k(\Lambda, u_0)$ has a probabilistic interpretation as a moment of some natural random variable associated to the interlacing sequence Λ ; we expect that the answer for this question is negative. We will use M_k purely as an auxiliary tool for studying the moments of the random variable $F_T(u_0)$, see below.

The right-hand side of (8.4) is very similar to its counterpart (8.1); the only difference is that the second sum on the right-hand side of (8.1) runs over certain sequences \mathbf{x} which *additionally* fulfill the condition (X) from Lemma 6.1(c).

Let us fix an integer $s \in \{0, \dots, \mathbb{L} + 1\}$ and consider the set $W_{s, \mathbb{L}}$ of interlacing sequences Λ of the form (8.3) with the property that $\mathbb{x}_0, \mathbb{x}_1, \dots, \mathbb{x}_{s-1} \leq u_0$ are all small and $\mathbb{x}_s, \dots, \mathbb{x}_{\mathbb{L}} > u_0$ are all big; in other words s is the cardinality of small entries of the set \mathbb{X} . Thanks to the aforementioned removal of the condition (X), the restriction of the function $\Lambda \mapsto M_k(\Lambda, u_0)$ to the set $W_{s, \mathbb{L}}$ is a rational function in the variables $\mathbb{x}_0, \dots, \mathbb{x}_{\mathbb{L}}, \mathbb{y}_1, \dots, \mathbb{y}_{\mathbb{L}}$. Our general strategy is to investigate this rational function M_k .

The price we have to pay for the aforementioned omission of the condition (X) is that the rational function M_k is singular in (some subset of) the set of non-generic interlacing sequences, in particular it is not clear how to evaluate $M_k(\Lambda, u_0)$ in the special case when the interlacing sequence Λ corresponds to a Young diagram λ (which is clearly non-generic). On the bright side, Lemma 8.1 below shows that there is a special way of taking the limit value of M_k at the singularity which provides a bridge with our main subject of investigations, the moment $m_k(F_T(u_0))$. In fact, from the proof of Theorem 3.2 it will follow that the aforementioned singularity is removable and thus an analogue of Lemma 8.1 holds true for *any* way of taking the limit $\Lambda \rightarrow \lambda$.

8.4. Regularization. Let a Young diagram λ be fixed and let Λ be the corresponding interlacing sequence. For $\epsilon > 0$ we define the interlacing sequence

$$\Lambda^\epsilon = (\mathbb{x}_0^\epsilon, \dots, \mathbb{x}_{\mathbb{L}}^\epsilon; \mathbb{y}_1^\epsilon, \dots, \mathbb{y}_{\mathbb{L}}^\epsilon)$$

given by

$$\mathbb{x}_j^\epsilon = \mathbb{x}_j + j\epsilon, \quad \mathbb{y}_j^\epsilon = \mathbb{y}_j + j\epsilon.$$

Note that if ϵ is small enough, the set of concave corners of Λ^ϵ is generic so that $M_k(\Lambda^\epsilon, u_0)$ is well-defined.

The distance

$$(8.5) \quad \mathbb{x}_j^\epsilon - \mathbb{y}_j^\epsilon = \mathbb{x}_j - \mathbb{y}_j$$

between any convex corner \mathbb{y}_j^ϵ and the next concave corner to the right \mathbb{x}_j^ϵ does not depend on the value of ϵ , and is a positive integer which has a natural interpretation for the original Young diagram λ , cf. Figure 9.

Lemma 8.1. *We suppose that u_0 is not an integer number. With the above notations, the moment m_k is equal to the limit of the moment M_k , when ϵ tends to zero:*

$$m_k(F_T(u_0)) = \lim_{\epsilon \rightarrow 0} M_k(\Lambda^\epsilon, u_0).$$

Proof. Let $s \in \{0, \dots, \mathbb{L} + 1\}$ be the cardinality of the small concave corners of λ ; with the notations of Section 8.3 this means that $\Lambda^\epsilon \in W_{s, \mathbb{L}}$ if $|\epsilon|$

is small enough. By writing $x_i = \mathbb{x}_{r_i}^\epsilon$ we may write (8.4) as

$$(8.6) \quad M_k(\Lambda^\epsilon, u_0) = k! \sum_{\mathbf{a} \in \mathcal{C}_n} \sum_{s \geq r_1 > \dots > r_\ell \geq 1} \Theta(\mathbb{x}_{r_1}^\epsilon, \dots, \mathbb{x}_{r_\ell}^\epsilon) \prod_{i=1}^{\ell} \frac{(-1)^{a_i-1}}{a_i} \mu_\Lambda(\mathbb{x}_{r_i}^\epsilon) \mathbf{G}_{\Lambda^\epsilon}^{a_i-1}(\mathbb{x}_{r_i}^\epsilon - 1).$$

Similarly (8.1) can be written as

$$(8.7) \quad m_k(F_T(u_0)) = k! \sum_{\mathbf{a} \in \mathcal{C}_n} \sum \Theta(\mathbb{x}_{r_1}, \dots, \mathbb{x}_{r_\ell}) \prod_{i=1}^{\ell} \frac{(-1)^{a_i-1}}{a_i} \mu_\Lambda(\mathbb{x}_{r_i}) \mathbf{G}_\Lambda^{a_i-1}(\mathbb{x}_{r_i} - 1);$$

the consequence of the condition (X) from Lemma 6.1 is that the second sum runs over $s \geq r_1 > \dots > r_\ell \geq 1$ which additionally fulfill

$$(8.8) \quad \mathbb{x}_{r_i} - \mathbb{y}_{r_i} \geq a_i \quad \text{for } i \in \{1, \dots, \ell\};$$

in the special case when $r_i = 0$ and \mathbb{y}_0 is not defined the above condition is fulfilled by convention.

Let us consider a summand of (8.6) which corresponds to $\mathbf{a} \in \mathcal{C}_n$ and a tuple (r_1, \dots, r_ℓ) for which (8.8) is *not* satisfied thus $1 \leq \mathbb{x}_{r_i} - \mathbb{y}_{r_i} \leq a_i - 1$ for some choice of the index i . One of the factors in $\mathbf{G}_{\Lambda^\epsilon}^{a_i-1}(\mathbb{x}_{r_i}^\epsilon - 1)$ is equal to

$$\mathbf{G}_{\Lambda^\epsilon}(\mathbb{x}_{r_i}^\epsilon - (\mathbb{x}_{r_i} - \mathbb{y}_{r_i})) = \mathbf{G}_{\Lambda^\epsilon}(\mathbb{x}_{r_i}^\epsilon - (\mathbb{x}_{r_i}^\epsilon - \mathbb{y}_{r_i}^\epsilon)) = \mathbf{G}_{\Lambda^\epsilon}(\mathbb{y}_{r_i}^\epsilon) = 0$$

by the very definition of the Cauchy transform; as a consequence the whole corresponding summand of (8.6) vanishes as well.

On the other hand, any summand in (8.6) for which (8.8) is satisfied is continuous at $\epsilon = 0$ and clearly converges as $\epsilon \rightarrow 0$ to its counterpart in (8.7) which completes the proof. \square

8.5. Cumulants for interlacing sequences. For a given interlacing sequence Λ and u_0 we consider the corresponding sequence of moments M_1, M_2, \dots with $M_k = M_k(\Lambda, u_0)$ given by (8.4). We revisit Section 3.3 and consider the corresponding sequence of formal cumulants K_1, K_2, \dots with $K_k = K_k(\Lambda, u_0)$ given by the expansion

$$\log \sum_{k=0}^{\infty} \frac{M_k}{k!} t^k = \sum_{k=1}^{\infty} K_k \frac{t^k}{k!}.$$

Since each cumulant K_k can be expressed as a polynomial in the moments M_1, \dots, M_k , Lemma 8.1 implies the following result.

Lemma 8.2. *Suppose that u_0 is not an integer number. With the above notations, the cumulants of the random variable $F_T(u_0)$ are given by*

$$\kappa_k(F_T(u_0)) = \lim_{\epsilon \rightarrow 0} K_k(\Lambda^\epsilon, u_0).$$

9. PROOF OF THEOREM 3.2

9.1. The graph expansion for the moments. Using Lemma 7.1 and the fact that for any integer $r \geq 1$

$$(9.1) \quad \mathbf{G}_\Lambda(x_i - r) = - \sum_{x_{i,r}} \frac{\mu_\Lambda(x_{i,r})}{x_{i,r} - x_i + r},$$

we may rewrite the formula (8.4) as follows.

Corollary 9.1. *If the interlacing sequence Λ is generic then the moment M_k is given by*

$$(9.2) \quad M_k(\Lambda, u_0) = k! \sum_{\mathbf{a} \in \text{Comp}_k} \sum_{x_\ell < \dots < x_1 \leq u_0} \prod_{i=1}^{\ell} \frac{\mu_\Lambda(x_i)}{a_i} \times \\ \prod_{r=1}^{a_i-1} \sum_{x_{i,r}} \frac{\mu_\Lambda(x_{i,r})}{x_{i,r} - x_i + r} \times \sum_{F \in \text{MS}_\ell} \frac{\beta_F}{\prod_{(i,j) \in E_F} (x_j - x_i + a_i)},$$

where $\ell = \ell(\mathbf{a})$ is the length of the composition \mathbf{a} . Recall that the constant β_F was defined in (7.2). The above sums run over $x_i, x_{i,r} \in \{\mathbb{X}_1, \dots, \mathbb{X}_\mathbb{L}\}$.

In the following we denote

$$x_{i,0} := x_i.$$

Now we will define multi-caterpillar graphs and with them we will simplify Corollary 9.1.

9.2. Multi-caterpillar graphs. By applying the distributive law to the right-hand side of (9.2) we obtain a sum of a lot of terms; to each of them we shall associate a certain directed weighted graph G . Each term is a product of

- the numerical factor

$$k! \beta_F \prod_{i=1}^{\ell} \frac{1}{a_i} \prod_{r \in \{0, \dots, a_i-1\}} \mu_\Lambda(x_{i,r})$$

for some multi-spine graph F , and

- the reciprocal of the product of the polynomials of the form

$$(x_{i,r} - x_{i,0} + r) \quad \text{or} \quad (x_{j,0} - x_{i,0} + a_j).$$

The latter product of polynomials is in our focus.

We create a *multi-caterpillar graph* G with k vertices as follows. We create ℓ black vertices and $k - \ell$ red vertices. The black vertices correspond to the variables $x_{1,0}, \dots, x_{\ell,0}$. For each $j \in \{1, \dots, \ell\}$ there are $a_j - 1$ red vertices connected with the black vertex $x_{j,0}$; they correspond to the variables $x_{j,1}, \dots, x_{j,a_j-1}$. We tag the vertices in such a way that the vertex which corresponds to the variable $x_{i,j}$ is tagged by the pair (i, j) . Each factor $(x_{i_2,j_2} - x_{i_1,j_1} + a)$ corresponds to the oriented edge with the weight a from the vertex tagged (i_1, j_1) to the vertex tagged (i_2, j_2) .

Example 9.2. The graph shown in Figure 24 was obtained from the term

$$\frac{1}{(x_{5,1} - x_5 + 1)(x_{5,2} - x_5 + 2)(x_{3,1} - x_3 + 1)(x_{2,1} - x_2 + 1)} \times \frac{1}{(x_5 - x_1 + 1)(x_4 - x_5 + 3)(x_3 - x_4 + 1)}$$

which is one of the summands in Corollary 9.1 which corresponds to $\mathbf{a} = (1, 2, 2, 1, 3)$. Figure 25 shows the same graph without the Young diagram.

9.3. Multi-caterpillar graphs, the formal approach. More formally, a *multi-caterpillar graph* G with tagged vertices is a directed, weighted graph with black and red vertices, for which there exists a tuple of integers $a_1, \dots, a_\ell \geq 1$ which fulfills the following properties.

Firstly, the subgraph composed of all black vertices and the edges between them forms a multi-spine graph with $\ell \geq 1$ vertices tagged $(1, 0), \dots, (\ell, 0)$. For each $j \in \{1, \dots, \ell\}$ the black vertex tagged $(j, 0)$ has at most one outgoing edge to another black vertex; if such an edge exists, its weight is equal to a_j .

Secondly, if we remove the edges between the black vertices, each connected component of the resulting graph consists of a single black vertex $(j, 0)$ for some value of $j \in \{1, \dots, \ell\}$, and $a_j - 1$ red vertices tagged $(j, 1), \dots, (j, a_j - 1)$. There are no connections between the red vertices; for each $k \in \{1, \dots, a_j - 1\}$ there is an oriented edge from the black vertex $(j, 0)$ to the red vertex (j, k) ; this edge carries the weight k .

By MC_k^{tag} we denote the set of all multi-caterpillar graphs with k tagged vertices.

9.4. Three systems of naming the vertices. In the following, we will have twice to use the technique of double counting. For this reason we will use the following three systems of naming the vertices in an oriented weighted graph with k vertices:

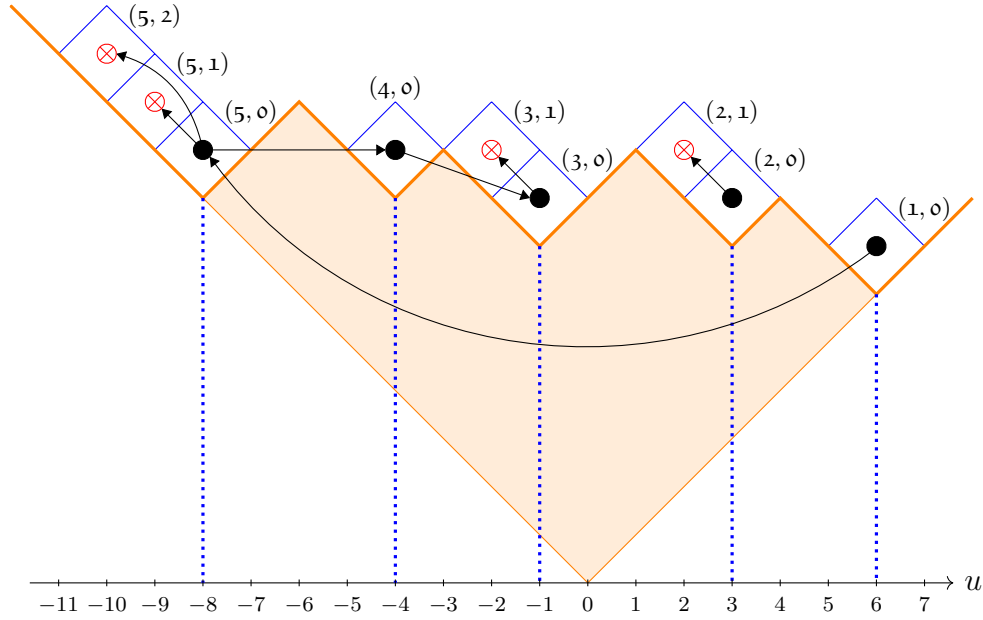


Figure 24. The multi-caterpillar graph considered in Example 9.2. The composition $\mathbf{a} = (1, 2, 2, 1, 3)$ was visualized as a configuration of white boxes which could occur in the anti-Pieri growth. The vertices of the multi-caterpillar graph (black vertices \bullet and red vertices \otimes) correspond to the boxes of the Young diagram where the Plancherel growth occurred. In order to improve visibility the weights of the edges were not shown.

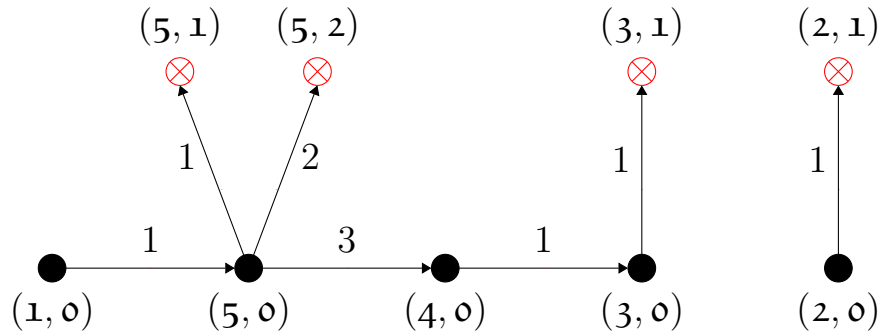


Figure 25. The multi-caterpillar graph from Figure 24 with the weights of the edges shown.

- the elements of the set $\mathbb{N} \times \mathbb{N}_0$ will be called *tags*; the naming of the vertices with tags (or, shortly, tagging) was used in Sections 9.2 and 9.3. An example of a graph with tagged vertices is shown in Figure 26a;
- the elements of the set $\{1, \dots, k\}$ will be called *labels*; we will consider only labelings with the property that if a pair of vertices $v_1, v_2 \in \{1, \dots, k\}$ is connected by an oriented edge $e = (v_1, v_2)$, its weight

$$(9.3) \quad w(e) = w(v_1, v_2) = v_2 - v_1$$

is equal to the difference of the vertex labels, see (3.6).

- by *marks* we understand the elements of an arbitrary fixed set which consists of k elements; in order to avoid confusion between marks and labels we may declare that the set of marks

$$(9.4) \quad \{\underline{1}, \underline{2}, \dots, \underline{k}\}$$

consists of k underlined integers. An example of a graph with marked vertices is shown in Figure 26b;

9.5. Black-decreasing decorations. Let G be a multi-caterpillar graph with tagged vertices. The decoration $\mathbf{x} \in D_G$ is called *black-decreasing* if for any pair of black vertices $(p, 0)$ and $(q, 0)$ with $p < q$ the corresponding values of the decoration fulfill $x_{p,0} > x_{q,0}$. The set of all black-decreasing decorations of a multi-caterpillar graph G will be denoted by $D_G^>$.

Using Corollary 9.1 we can write the moment $M_k(\Lambda, u_0)$ as a sum over multi-caterpillar graphs, as follows. We replace the double sum in (9.2) over compositions and over multi-spine graphs by the sum over multi-caterpillar graphs $G \in \text{MC}_k^{\text{tag}}$. In addition, we replace the sum over the variables (x_i) and $(x_{i,r})$ by the sum over black-decreasing decorations. It follows that

$$(9.5) \quad M_k = k! \sum_{G \in \text{MC}_k^{\text{tag}}} \sum_{\mathbf{x} \in D_G^>} \alpha_G f_G,$$

where the constant α_G is defined as

$$(9.6) \quad \alpha_G = (-1)^{|B_G|} \left(\prod_{(i,j) \in V_G} \mu_\Lambda(x_{i,j}) \right) \left(\prod_{G'} \frac{-1}{|V_{G'}|} \right),$$

where G' runs over all connected components of the graph G . Note that α_G depends also on the choice of the decoration \mathbf{x} ; in order to keep the notation lightweight we will make this dependence implicit.

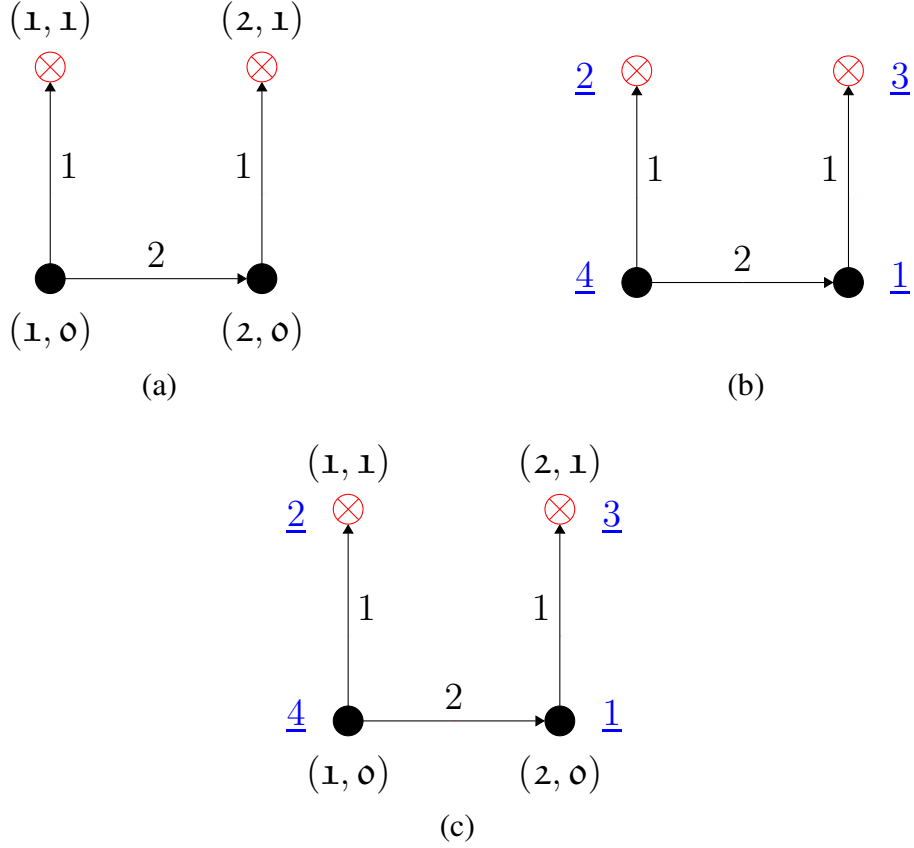


Figure 26. Examples of multi-caterpillar graphs: (a) with tagged vertices; the tags are printed black and belong to the set $\{(1, 0), (1, 1), (2, 0), (2, 1)\}$, (b) with marked vertices; the marks are printed blue and belong to the set $\{\underline{1}, \underline{2}, \underline{3}, \underline{4}\}$, (c) with tagged and marked vertices.

9.6. Double counting. Let MC_k^{mark} denote the set of multi-caterpillar graphs with k marked vertices, i.e., the set of weighted and oriented graphs G with the vertex set $\{\underline{1}, \dots, \underline{k}\}$ such that there exists a way to tag the vertices in such a way that G becomes a multi-caterpillar graph with k tagged vertices in the sense considered in Section 9.3. Let MC_k^{tm} denote the set of multi-caterpillar graphs with k vertices which are simultaneously tagged and marked. Examples of such graphs are shown in Figure 26.

For any graph $G \in MC_k^{\text{tag}}$ we have $k!$ ways to mark its k vertices by the elements of (9.4).

Let G be a graph. Its decoration $\mathbf{x} \in D_G$ is called *black-injective* if $x_i \neq x_j$ for all pairs of black vertices $i, j \in B_G$ such that $i \neq j$. We denote the set of all black-injective decorations of G by D_G^\neq , and the set of non-black-injective decorations of G by $D_G^\equiv = D_G \setminus D_G^\neq$.

Moreover, for each black-injective decoration \mathbf{x} of $G \in \text{MC}_k^{\text{mark}}$ we can tag the vertices of G in a canonical way as follows. We tag the black vertices by $(1, 0), (2, 0), \dots$ in the opposite order to the one given by the decoration \mathbf{x} . Next, for each black vertex b with the tag $(j, 0)$ we tag the white vertices connected with b by $(j, 1), (j, 2), \dots$ according to the increasing order of their corresponding weight of edges. In this way G becomes a caterpillar graph with tagged vertices, and \mathbf{x} becomes a decreasing decoration.

Using these two observations and (9.5), we obtain

$$\begin{aligned}
 (9.7) \quad M_k &= k! \sum_{G \in \text{MC}_k^{\text{tag}}} \sum_{\mathbf{x} \in D_G^\neq} \alpha_G f_G \\
 &= \sum_{G \in \text{MC}_k^{\text{tm}}} \sum_{\mathbf{x} \in D_G^\neq} \alpha_G f_G \\
 &= \sum_{G \in \text{MC}_k^{\text{mark}}} \sum_{\mathbf{x} \in D_G^\neq} \alpha_G f_G.
 \end{aligned}$$

The constant α_G was defined in (9.6).

9.7. Sum over all decorations.

Proposition 9.3. *The following double sum over multi-caterpillar graphs and their decorations remains the same when we restrict the sum to black-injective decorations, i.e., for each integer $k \geq 1$,*

$$(9.8) \quad \sum_{G \in \text{MC}_k^{\text{mark}}} \sum_{\mathbf{x} \in D_G} \alpha_G f_G = \sum_{G \in \text{MC}_k^{\text{mark}}} \sum_{\mathbf{x} \in D_G^\neq} \alpha_G f_G.$$

Proof. We consider the difference of the left-hand side and the right-hand side of (9.8)

$$(9.9) \quad \Delta = \sum_{G \in \text{MC}_k^{\text{mark}}} \sum_{\mathbf{x} \in D_G^\equiv} \alpha_G f_G.$$

Our goal is to prove that $\Delta = 0$.

Let k be a fixed natural number, and let $B = \{b_1, \dots, b_l\} \subseteq \{\underline{1}, \dots, \underline{k}\}$ be a fixed set. Let $\text{MS}(B)$ denote the set of all multi-spine graphs F with the vertex set $V_F = B$. In particular $\text{MS}(\{\underline{1}, \dots, \underline{k}\}) = \text{MS}_k$. Let $\mathcal{G}_k^{\text{MC}}(B)$ denote the set of all multi-caterpillar graphs $G_\emptyset \in \text{MC}_k^{\text{mark}}$ with k marked vertices $\underline{1}, \dots, \underline{k}$ such that

- the set of black vertices of G_\emptyset is given by $B_{G_\emptyset} = B$, and
- there is no edge in G_\emptyset connecting two black vertices.

Let k be a fixed natural number. Every multi-caterpillar graph $G \in \text{MC}_k^{\text{mark}}$ can be decomposed in a unique way into the union of two graphs $G_\emptyset \in \mathcal{G}_k^{\text{MC}}(B_G)$ and $F \in \text{MS}(B_G)$. In other words, the graph F is the graph composed of all black vertices of the graph G and the edges between them, and the graph G_\emptyset is the graph composed of all vertices of the graph G and the remaining edges. Furthermore, for each vertex $v \in V_F$ of the graph F we define the number a_v as the number of vertices in the connected component of the graph G_\emptyset which contains the vertex v . With the notations from Lemma 7.1, the constant β_F given by (7.2) is equal to

$$(9.10) \quad \beta_F = (-1)^{|V_F|} \frac{\prod_{v \in V_F} a_v}{\prod_{G'} [(-1)^{|V_{G'}|}]},$$

where the product over G' runs over all connected components of the graph G . In addition, for each edge $e = (i, j) \in E_F$ we define its weight as $w(e) = a_i$.

Now we define the constant γ_{G_\emptyset} so that

$$\alpha_G = \beta_F \gamma_{G_\emptyset}.$$

From (9.6) and (9.10) we obtain that the constant

$$\gamma_{G_\emptyset} = \frac{\alpha_G}{\beta_F} = \frac{\prod_{v \in V_{G_\emptyset}} \mu_\Lambda(x_v)}{\prod_{v \in B_{G_\emptyset}} a_v}$$

depends only on the graph G_\emptyset and the decoration \mathbf{x} .

In addition, for any set $B \subseteq \{\underline{1}, \dots, \underline{k}\}$ the union of each pair of graphs $G_\emptyset \in \mathcal{G}_k^{\text{MC}}(B)$ and $F \in \text{MS}(B)$ as above is a multi-caterpillar graph with k marked vertices. Therefore, we can replace the sum in (9.9) over all multi-caterpillar graphs with marked vertices by a triple sum over all possible sets of black vertices, over multi-caterpillar graphs, and over all multi-spine graphs. It follows that

$$\begin{aligned} \Delta &= \sum_{B \subseteq \{\underline{1}, \dots, \underline{k}\}} \sum_{\substack{G \in \text{MC}_k^{\text{mark}} \\ B_G = B}} \sum_{\mathbf{x} \in D_G^-} \alpha_G f_G \\ &= \sum_{B \subseteq \{\underline{1}, \dots, \underline{k}\}} \sum_{G_\emptyset \in \mathcal{G}_k^{\text{MC}}(B)} \sum_{\mathbf{x} \in D_{G_\emptyset}^-} \gamma_{G_\emptyset} f_{G_\emptyset} \sum_{F \in \text{MS}(B)} \beta_F f_F. \end{aligned}$$

Let $B = \{b_1, \dots, b_l\} \subseteq \{\underline{1}, \dots, \underline{k}\}$ be a fixed set and $\mathbf{x}_B = (x_{b_1}, \dots, x_{b_l})$ be a fixed non-black-injective decoration of B . Using the formula (7.1)

(e.g., by temporarily renumbering the vertices b_1, \dots, b_l into $1, \dots, l$), we obtain that the internal sum is equal to

$$\sum_{F \in \text{MS}(B)} \beta_F f_F(x_{b_1}, \dots, x_{b_l}) = \Theta(x_{b_1}, \dots, x_{b_l}) = 0$$

since at least one of the factors in the numerator of Θ is equal to zero. (Recall that the definition of Θ was given in (6.3).) Thus $\Delta = 0$ as required. \square

9.8. The first formula for the cumulants. We denote by $C_k^{\text{mark}} \subset \text{MC}_k^{\text{mark}}$ the set of *connected multi-caterpillar graphs with k marked vertices*. Its elements will be called *caterpillar graphs with k marked vertices*.

Using Proposition 9.3 we transform the formula (9.7) to

$$M_k = \sum_{G \in \text{MC}_k^{\text{mark}}} \sum_{\mathbf{x} \in D_G} \alpha_G f_G.$$

We can look separately at each connected component G' of a multi-caterpillar graph G . The connected components correspond to the blocks of a set-partition. Thus

$$\begin{aligned} (9.11) \quad M_k &= \sum_{G \in \text{MC}_k^{\text{mark}}} \sum_{\mathbf{x} \in D_G} \alpha_G f_G \\ &= \sum_{G \in \text{MC}_k^{\text{mark}}} \prod_{G'} \sum_{\mathbf{x} \in D_{G'}} \alpha_{G'} f_{G'} \\ &= \sum_{\pi} \prod_{b \in \pi} \sum_{G' \in C_b^{\text{mark}}} \sum_{\mathbf{x} \in D_{G'}} \alpha_{G'} f_{G'} \\ &= \sum_{\pi} \prod_{b \in \pi} \tilde{K}_{|b|}, \end{aligned}$$

where π runs over all set-partitions of the set $\{\underline{1}, \dots, \underline{k}\}$, and b runs over all blocks of π . Above \tilde{K}_j is defined as

$$\begin{aligned} (9.12) \quad \tilde{K}_j &:= \sum_{G \in C_j^{\text{mark}}} \sum_{\mathbf{x} \in D_G} \alpha_G f_G \\ &= \frac{1}{j} \sum_{G \in C_j^{\text{mark}}} \sum_{\mathbf{x} \in D_G} \left(\prod_{v \in V_G} \mu_{\Lambda}(x_v) \right) (-1)^{|B_G|-1} f_G. \end{aligned}$$

In our setting the moment-cumulant formula (3.2) takes the form

$$M_k = \sum_{\pi \in \Pi_k} \prod_{b \in \pi} K_{|b|}.$$

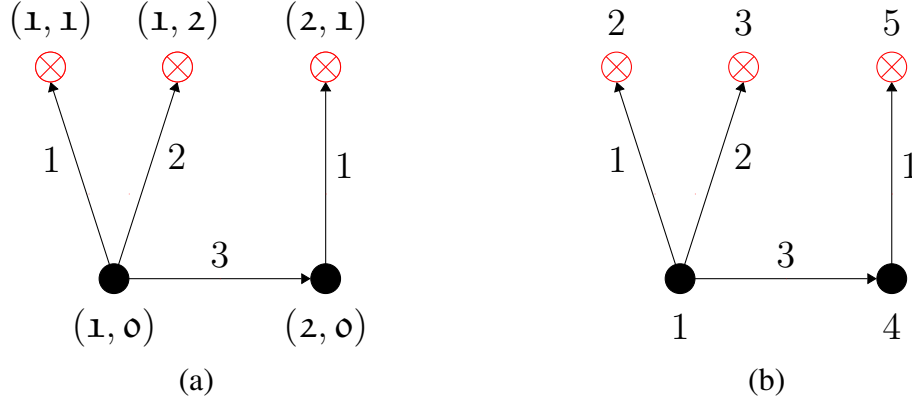


Figure 27. (a) A caterpillar graph with tagged vertices.
 (b) The same graph with labeled vertices. The labels belong to the set $\{1, 2, 3, 4, 5\}$.

(Here π still runs over set-partitions, and b runs over all blocks of π .) It can be viewed as a system of algebraic equations for the unknowns (K_k) . This system of equations has an upper-triangular form in the sense that the k -th equation allows us to express the cumulant K_k as the sum of the moment M_k and some complicated polynomial in the variables K_1, \dots, K_{k-1} . Such a system of equations can be solved recursively and clearly has a unique equation. Equation (9.11) shows that the sequence (\tilde{K}_k) is a solution of this system of equations; since the solution is unique, it follows that the cumulant

$$K_k = \tilde{K}_k$$

is given by (9.12) after the substitution $j = k$.

9.9. Caterpillar graphs with labeled vertices. We say that a connected, weighted, oriented graph G is a *caterpillar graph with k labeled vertices* if its vertex set is equal to $\{1, \dots, k\}$, the weights of the edges fulfill the convention (9.3), and there exists some way of tagging the vertices of G in such a way that G becomes an element of MC_k^{tag} , see Section 9.3. An example of a caterpillar graph with labeled vertices is given in Figure 27b. The set of caterpillar graphs with k labeled vertices will be denoted by C_k^{lab} . This definition may sound a bit abstract so we provide an alternative description below.

Note that for any connected of a graph $G \in \text{MC}_k^{\text{tag}}$ there is a unique way of labeling the vertices so that the requirement (9.3) is fulfilled, given as follows. We start by assigning the number 1 to the unique black vertex with no incoming edges. Then, in the order given by the weights of the edges,

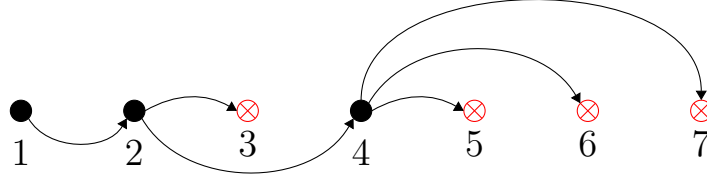


Figure 28. An example of a caterpillar graph with $k = 7$ labeled vertices. With the notations of (9.13) we have $\ell = 3$ black vertices and $b_1 = 1, b_2 = 2, b_3 = 4$; additionally we use the convention that $b_4 = 8$. The weights of the edges were not shown.

we number all endpoints of the edges outgoing from this vertex number 1 by successive natural numbers. We repeat the process at the unique black endpoint of an edge outgoing from 1, and continue until we visit all black vertices. In this way for any edge $e = (v_1, v_2)$ its weight is equal to the difference of the labels of the endpoints: $w(e) = v_2 - v_1$. The outcome is clearly an element of C_k^{lab} , and each element of C_k^{lab} can be obtained in this way.

The above procedure shows that the elements of C_k^{lab} can be characterized as follows. For each $G \in C_k^{\text{lab}}$ with the set of black vertices

$$(9.13) \quad B_G = \{b_1, \dots, b_\ell\} \subseteq \{1, \dots, k\}, \quad b_1 < \dots < b_\ell$$

we have that $\ell \geq 1$ and $b_1 = 1$. We will use the convention that $b_{\ell+1} = k+1$. The black vertices are connected by a series of oriented edges

$$(b_1, b_2), \quad (b_2, b_3), \quad \dots, \quad (b_{\ell-1}, b_\ell).$$

Additionally, each black vertex b_i (with $i \in \{1, \dots, \ell\}$) is connected to the red vertices $b_i + 1, b_i + 2, \dots, b_{i+1} - 1$ which immediate follow it by a collection of oriented edges

$$(b_i, b_i + 1), \quad (b_i, b_i + 2), \quad \dots, \quad (b_i, b_{i+1} - 1),$$

see Figure 28 for an example.

In particular, since the structure of a caterpillar graph with labeled vertices is determined by its set of black vertices, it follows that $|C_k^{\text{lab}}| = 2^{k-1}$.

9.10. The second formula for the cumulants. We continue the discussion from Section 9.8 and revisit the formula (9.12) for the cumulant K_k . As we already mentioned, the connected graph $G \in C_k^{\text{mark}}$ can be labeled in a unique way so that it becomes an element of C_k^{lab} . On the other hand, for each graph $G \in C_k^{\text{lab}}$, there exist $k!$ ways to mark the vertices so that the

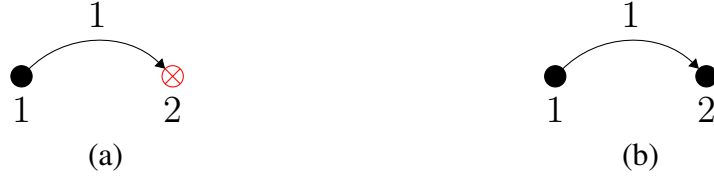


Figure 29. (a) Caterpillar graph with one black and one red vertices. (b) Caterpillar graph with two black vertices.

outcome is a caterpillar graph with k marked vertices. In this way we proved the following intermediate result.

Corollary 9.4. *Let Λ be an interlacing sequence with a generic set of concave corners. For each $u_0 \in \mathbb{R}$ the n -th formal cumulant considered in Section 8.5 is given by the following sum over caterpillar graphs with k labeled vertices*

$$(9.14) \quad K_k = (k-1)! \sum_{G \in C_k^{\text{lab}}} \sum_{\mathbf{x} \in D_G} (-1)^{|B_G|-1} f_G \prod_{j \in \{1, \dots, k\}} \mu_\Lambda(x_j).$$

For example, for $k = 2$ we obtain

$$K_2 = \sum_{x_1 \leq u_0} \sum_{x_2} \frac{\mu_\Lambda(x_1) \mu_\Lambda(x_2)}{x_2 - x_1 + 1} - \sum_{x_1 \leq u_0} \sum_{x_2 \leq u_0} \frac{\mu_\Lambda(x_1) \mu_\Lambda(x_2)}{x_2 - x_1 + 1}.$$

The first summand corresponds to the caterpillar graph shown of Figure 29a, and the second summand corresponds to the caterpillar graph shown of Figure 29b.

9.11. Sum over non-crossing alternating trees.

Proposition 9.5. *Let Λ be an interlacing sequence with a generic set of concave corners. For each $u_0 \in \mathbb{R}$ the n -th formal cumulant considered in Section 8.5 is given by the following sum over noncrossing alternating trees*

$$(9.15) \quad K_k = (k-1)! \sum_{H \in \mathbb{T}_k} \sum_{\mathbf{x} \in D_H} (-1)^{|B_H|-1} f_H \prod_{j \in \{1, \dots, k\}} \mu_\Lambda(x_j).$$

Proof. In (9.14) we can reverse the order of the sums and write

$$K_k = -(k-1)! \sum_{x_1, \dots, x_k \in \mathbb{X}} \mathfrak{C}_k(x_1, \dots, x_k) \prod_{j \in \{1, \dots, k\}} \mu_\Lambda(x_j),$$

where

$$\mathfrak{C}_k(x_1, \dots, x_k) := \sum_{\substack{G \in C_k^{\text{lab}} \\ (x_1, \dots, x_k) \in D_G}} (-1)^{|B_G|} f_G(x_1, \dots, x_k).$$

Similarly, the right-hand side of (9.15) can be written as

$$-(k-1)! \sum_{x_1, \dots, x_k \in \mathbb{X}} \mathfrak{T}_k(x_1, \dots, x_k) \prod_{j \in \{1, \dots, k\}} \mu_\Lambda(x_j),$$

where

$$\mathfrak{T}_k(x_1, \dots, x_k) := \sum_{\substack{H \in \mathbb{T}_k \\ (x_1, \dots, x_k) \in D_H}} (-1)^{|B_H|} f_H(x_1, \dots, x_k).$$

As a side remark note that $\mathfrak{T}_k(x_1, \dots, x_k)$ is a quantity which (up to a scaling factor) is closely related to the random variable Z from Remark 3.4. The result is a consequence of Lemma 9.6 below. \square

Lemma 9.6. *With the above notations,*

$$\mathfrak{C}_k(x_1, \dots, x_k) = \mathfrak{T}_k(x_1, \dots, x_k)$$

holds true for any $k \geq 1$ and any $x_1, \dots, x_k \in \mathbb{R}$ for which the left-hand side of the equality does not involve division by zero.

Proof. In the special case $k = 1$ we have that the set of graphs $C_1^{\text{lab}} = \mathbb{T}_1$ which contributes to $\mathfrak{C}_1(x_1)$, respectively to $\mathfrak{T}_1(x_1)$, consists of a single element depicted in Figure 14a. Thus

$$\mathfrak{C}_1(x_1) = \mathfrak{T}_1(x_1) = \begin{cases} -1 & \text{if } x_1 \leq u_0, \\ 0 & \text{if } x_1 > u_0. \end{cases}$$

Let $k \geq 2$. In the case when $x_k \leq u_0$ we obtain that

$$\mathfrak{T}_{x_1, \dots, x_k} = 0$$

because the rightmost vertex of any non-crossing alternating tree $H \in \mathbb{T}_k$ is white thus (x_1, \dots, x_k) is not a decoration of H and the sum runs over the empty set.

Let $C^{\text{lab}}(V)$ and $\mathbb{T}(V)$ denote, respectively, the set of caterpillar graphs and the set of non-crossing alternating trees such that their vertex set is equal to V . In particular $C^{\text{lab}}(\{1, \dots, k\}) = C_k^{\text{lab}}$ and $\mathbb{T}(\{1, \dots, k\}) = \mathbb{T}_k$ for any natural number k .

Let $H \in \mathbb{T}_k$ be a non-crossing alternating tree with k vertices. Obviously H contains the edge $e = (1, k)$ connecting the leftmost and the rightmost vertex. After removing the edge e from the graph H , the resulting graph $H \setminus e$ has two connected components: $H_1 \in \mathbb{T}_{i-1}(\{1, \dots, i-1\})$ and $H_2 \in \mathbb{T}_{k-i}(\{i, \dots, k\})$ for some $i \in \{2, \dots, k\}$. In the special case when the graph H_2 consists of a single (white) vertex, we change its color to black. This way, each non-crossing alternating tree with the vertex set

$\{1, \dots, k\}$ decomposes uniquely into a sum of the edge e and two non-crossing alternating trees H_1 with the vertex set $\{1, \dots, i-1\}$ and H_2 with the vertex set $\{i, \dots, k\}$.

If $i \neq k$ then (x_1, \dots, x_k) is a decoration of H if and only if the prefix (x_1, \dots, x_{i-1}) is a decoration of H_1 and the suffix (x_i, \dots, x_k) is a decoration of H_2 ; the special case when $i = k$ and the tree H_2 consists of a single vertex has to be considered separately. Therefore we obtain the following recurrence relation:

$$\mathfrak{T}_k(x_1, \dots, x_k) = \begin{cases} 0 & \text{if } x_k \leq u_0, \\ \sum_{i=2}^{k-1} \frac{\mathfrak{T}_{i-1}(x_1, \dots, x_{i-1}) \mathfrak{T}_{k-i+1}(x_i, \dots, x_k)}{x_k - x_1 + k - 1} & \\ + \frac{\mathfrak{T}_{k-1}(x_1, \dots, x_{k-1})}{x_k - x_1 + k - 1} & \text{if } x_k > u_0. \end{cases}$$

We will prove that the sequence of functions \mathfrak{C}_k satisfies the same recurrence relation.

If $k \geq 2$ and $x_k \leq u_0$ then $\mathfrak{C}(x_1, \dots, x_k) = 0$ because we can pair caterpillar graphs from C_k^{lab} into pairs that differ only in the color of the far-right vertex, and the contribution of each pair to the sum is zero.

Let $k \geq 2$ be a natural number, let $x_k > u_0$ and let $G \in C_k^{\text{lab}}$ be a caterpillar graph. There is a unique path (i_1, \dots, i_t) with $t \geq 2$ from the vertex 1 to the vertex k which means that $i_1 = 1$ and $i_t = k$, and $(i_1, i_2), (i_2, i_3), \dots, (i_{t-1}, i_t) \in E_G$. In the special case when $e = (1, k) \in E_G$, we have $t = 2$ and $e_1 = e$. Using the telescopic sum

$$x_k - x_1 + k - 1 = \sum_{j=1}^{t-1} (x_{i_{j+1}} - x_{i_j} + i_{j+1} - i_j)$$

we obtain

$$\begin{aligned} f_G(x_1, \dots, x_k) &= \sum_{j=1}^{t-1} \frac{x_{i_{j+1}} - x_{i_j} + i_{j+1} - i_j}{x_k - x_1 + k - 1} f_G(x_1, \dots, x_k) \\ &= \sum_{j=1}^{t-1} \frac{f_{G \setminus e_j}(x_1, \dots, x_k)}{x_k - x_1 + k - 1}, \end{aligned}$$

where $G \setminus e_j$ denotes the graph G with the edge e_j removed. Therefore,

$$\mathfrak{C}(x_1, \dots, x_k) = \sum_{\substack{G \in C_k^{\text{lab}} \\ (x_1, \dots, x_k) \in D_G}} (-1)^{|B_G|} \sum_{j=1}^{t-1} \frac{f_{G \setminus e_j}(x_1, \dots, x_k)}{x_k - x_1 + k - 1}.$$

In addition, every graph $G \in C_k^{\text{lab}}$ after removing any edge e_j splits in a unique way into the sum of two caterpillar graphs $G_1 \in C_{i-1}^{\text{lab}}(\{1, \dots, i-1\})$ and $G_2 \in C_{k-i+1}^{\text{lab}}(\{i, \dots, k\})$ for some $i \in \{2, \dots, k\}$. In the special case when $i = k$ and the graph G_2 consists a single (red) vertex, we change its color to black; this case will require separate analysis. In this way we can write $\mathfrak{C}(x_1, \dots, x_k)$ as a triple sum over all possible choices of the number i , over all graphs $G_1 \in C_{i-1}^{\text{lab}}(\{1, \dots, i-1\})$ and over all graphs $G_2 \in C_{k-i+1}^{\text{lab}}(\{i, \dots, k\})$, i.e.,

$$\begin{aligned} \mathfrak{C}(x_1, \dots, x_k) &= \sum_{i=2}^{k-1} \sum_{\substack{G_1 \in C_{i-1}^{\text{lab}}(\{1, \dots, i-1\}) \\ (x_1, \dots, x_{i-1}) \in D_{G_1}}} \sum_{\substack{G_2 \in C_{k-i+1}^{\text{lab}}(\{i, \dots, k\}) \\ (x_i, \dots, x_k) \in D_{G_2}}} \frac{(-1)^{|B_{G_1}|+|B_{G_2}|} f_{G_1} f_{G_2}}{x_k - x_1 + k - 1} \\ &\quad + \sum_{\substack{G_1 \in C_{i-1}^{\text{lab}}(\{1, \dots, k-1\}) \\ B_{G_1} \subseteq B}} \frac{(-1)^{|B_{G_1}|} f_{G_1}}{x_k - x_1 + k - 1} \\ &= \sum_{i=2}^{k-1} \frac{\mathfrak{C}_{i-1}(x_1, \dots, x_{i-1}) \mathfrak{C}_{k-i+1}(x_i, \dots, x_k)}{x_k - x_1 + k - 1} + \frac{\mathfrak{C}_{k-1}(x_1, \dots, x_{k-1})}{x_k - x_1 + k - 1} \end{aligned}$$

if $x_k > u_0$.

The sequences of rational functions \mathfrak{C}_k and \mathfrak{T}_k satisfy the same recurrence relation and have the same initial condition, which completes the proof. \square

9.12. Proof of Theorem 3.2.

Proof of Theorem 3.2. When the number u_0 is not an integer, we apply Lemma 8.2 and evaluate the cumulant $K_k(\Lambda^\epsilon, u_0)$ using Proposition 9.5.

However, when the number u_0 is an integer, the theorem is satisfied for any number $u \in (u_0, u_0 + 1)$, as shown above. Since $F_T(u_0)$ is a right-continuous function, then

$$F_T(u_0) = \lim_{u \rightarrow u_0} F_T(u),$$

and Theorem 3.2 also holds for the number u_0 . \square

10. ACKNOWLEDGMENTS

Research was supported by Narodowe Centrum Nauki, grant number 2017/26/A/ST1/00189. Additionally, the first named author was supported by Narodowe Centrum Badań i Rozwoju, grant number POWR.03.05.00-00-Z302/17-00.

We thank Márton Balázs, Gaetan Borot, Marek Bożejko, Maciej Dołęga, Pablo Ferrari, Patrik Ferrari, Mustazee Rahman, and Dan Romik for discussions and suggestions concerning the bibliography.

We thank Maciej Hendzel for performing some Monte Carlo experiments related to Conjecture 1.5.

REFERENCES

- [Aza20] Iskander Azangulov. “Distribution of fluctuations of Bernoulli system P -tableaux under RSK mapping”. In Russian. Private communication. Bachelor’s Thesis. Saint Petersburg State University, 2020.
- [BDJ99] J. Baik, P. Deift, and K. Johansson. “On the distribution of the length of the longest increasing subsequence of random permutations”. In: *J. Amer. Math. Soc.* 12 (1999), pp. 1119–1178.
- [BS07] Leonid V. Bogachev and Zhonggen Su. “Gaussian fluctuations of Young diagrams under the Plancherel measure”. In: *Proc. R. Soc. Lond. Ser. A Math. Phys. Eng. Sci.* 463.2080 (2007), pp. 1069–1080. DOI: 10.1098/rspa.2006.1808.
- [Fel68] William Feller. *An introduction to probability theory and its applications. Vol. I.* Third. John Wiley & Sons, Inc., New York-London-Sydney, 1968, pp. xviii+509.
- [FMP09] P. A. Ferrari, J. B. Martin, and L. P. R. Pimentel. “A phase transition for competition interfaces”. In: *Ann. Appl. Probab.* 19.1 (2009), pp. 281–317. DOI: 10.1214/08-AAP542.
- [Ful97] W. Fulton. *Young Tableaux: With Applications to Representation theory and Geometry.* Vol. 35. London Mathematical Society Student Texts. Cambridge: Cambridge University Press, 1997, pp. x+260.
- [GGP97] Israel M. Gelfand, Mark I. Graev, and Alexander Postnikov. “Combinatorics of hypergeometric functions associated with positive roots”. In: *The Arnold-Gelfand mathematical seminars.* Birkhäuser Boston, Boston, MA, 1997, pp. 205–221. DOI: 10.1007/978-1-4612-4122-5_10
- [GR19] Vadim Gorin and Mustazee Rahman. “Random sorting networks: local statistics via random matrix laws”. In: *Probab. Theory Related Fields* 175.1-2 (2019), pp. 45–96. DOI: 10.1007/s00440-018-0886-1.
- [Gus05] Jonas Gustavsson. “Gaussian fluctuations of eigenvalues in the GUE”. In: *Ann. Inst. H. Poincaré Probab. Statist.* 41.2 (2005), pp. 151–178. DOI: 10.1016/j.anihpb.2004.04.002.

- [Ker03] S. V. Kerov. *Asymptotic representation theory of the symmetric group and its applications in analysis*. Vol. 219. Translations of Mathematical Monographs. Translated from the Russian manuscript by N. V. Tsilevich, With a foreword by A. Vershik and comments by G. Olshanski. American Mathematical Society, Providence, RI, 2003, pp. xvi+201. DOI: 10.1090/mmono/219.
- [Ker93] S. Kerov. “Transition probabilities for continual Young diagrams and the Markov moment problem.” In: *Funct. Anal. Appl.* 27 (1993), pp. 104–117.
- [KV86] S. V. Kerov and A. M. Vershik. “The characters of the infinite symmetric group and probability properties of the Robinson-Schensted-Knuth algorithm”. In: *SIAM J. on Algebraic and Discrete Methods* 7.1 (1986), pp. 116–124. DOI: 10.1137/0607014.
- [LH02] Steffen L. Lauritzen and A. Hald. *Thiele: pioneer in statistics*. Thiele’s papers translated from the Danish by Steffen L. Lauritzen, With appreciations of Thiele’s work by Lauritzen and A. Hald. Oxford University Press, New York, 2002, pp. viii+264. DOI: 10.1093/acprof:oso/9780198509721.001.0001.
- [LS77] B. F. Logan and L. A. Shepp. “A variational problem for random Young tableaux”. In: *Advances in Math.* 26.2 (1977), pp. 206–222.
- [Mar16] Philippe Marchal. “Rectangular Young tableaux and the Jacobi ensemble”. In: *28th International Conference on Formal Power Series and Algebraic Combinatorics (FPSAC 2016)*. Discrete Math. Theor. Comput. Sci. Proc., BC. Assoc. Discrete Math. Theor. Comput. Sci., Nancy, 2016, pp. 839–850.
- [MMŚ23] Mikołaj Marciniak, Łukasz Maślanka, and Piotr Śniady. “Poisson limit theorems for the Robinson—Schensted correspondence and for the multi-line Hammersley process”. In: *Advances in Applied Mathematics* 145 (2023), p. 102478. DOI: <https://doi.org/10.1016/j.aam.2023.102478>.
- [MS17] James A. Mingo and Roland Speicher. *Free probability and random matrices*. Vol. 35. Fields Institute Monographs. Springer, New York; Fields Institute for Research in Mathematical Sciences, Toronto, 2017, pp. xiv+336. DOI: 10.1007/978-1-4939-6942-5.
- [Oko00] Andrei Okounkov. “Random matrices and random permutations”. In: *Internat. Math. Res. Notices* 20 (2000), pp. 1043–1095. DOI: 10.1155/S1073792800000532.
- [PR07] Boris Pittel and Dan Romik. “Limit shapes for random square Young tableaux”. In: *Adv. in Appl. Math.* 38.2 (2007), pp. 164–209. DOI: 10.1016/j.aam.2005.12.005.

- [Rom15] Dan Romik. *The surprising mathematics of longest increasing subsequences*. Vol. 4. Institute of Mathematical Statistics Textbooks. Cambridge University Press, New York, 2015, pp. xi+353.
- [Ros81] H. Rost. “Nonequilibrium behaviour of a many particle process: density profile and local equilibria”. In: *Z. Wahrsch. Verw. Gebiete* 58.1 (1981), pp. 41–53. DOI: 10.1007/BF00536194.
- [RŚ15] Dan Romik and Piotr Śniady. “Jeu de taquin dynamics on infinite Young tableaux and second class particles”. In: *Ann. Probab.* 43.2 (2015), pp. 682–737. DOI: 10.1214/13-AOP873.
- [RV21] Mustazee Rahman and Balint Virag. *Infinite geodesics, competition interfaces and the second class particle in the scaling limit*. preprint arXiv:2112.06849. 2021. DOI: 10.48550/ARXIV.2112.06849.
- [Sch59] Samuel Schechter. “On the Inversion of Certain Matrices”. In: *Mathematics of Computation - Math. Comput.* 13 (Apr. 1959), pp. 73–73. DOI: 10.1090/S0025-5718-1959-0105798-2.
- [Sta99] R. P. Stanley. *Enumerative combinatorics*. Vol. 2. Vol. 62. Cambridge Studies in Advanced Mathematics. Cambridge: Cambridge University Press, 1999, pp. xii+581. DOI: 10.1017/CBO9780511609589.
- [Tho64] Elmar Thoma. “Die unzerlegbaren, positiv-definiten Klassenfunktionen der abzählbar unendlichen, symmetrischen Gruppe”. In: *Math. Z.* 85 (1964), pp. 40–61. DOI: 10.1007/BF01114877.
- [VDK19] N. N. Vassiliev, V. S. Duzhin, and A. D. Kuzmin. “Investigation of properties of equivalence classes of permutations by inverse Robinson–Schensted –Knuth transformation”. In: *Information and Control Systems* 98.1 (June 2019), pp. 11–22. DOI: 10.31799/1684-8853-2019-1-11-22.
- [VK77] A. M. Vershik and S. V. Kerov. “Asymptotics of the Plancherel measure of the symmetric group and the limit form of Young tableaux”. In: *Soviet Math. Dokl.* 18 (1977), pp. 527–531.
- [VK81] A. M. Vershik and S. V. Kerov. “Asymptotic theory of the characters of a symmetric group”. In: *Funktsional. Anal. i Prilozhen.* 15.4 (1981), pp. 15–27, 96.
- [Voi94] Dan Voiculescu. “The analogues of entropy and of Fisher’s information measure in free probability theory. II”. In: *Invent. Math.* 118.3 (1994), pp. 411–440. DOI: 10.1007/BF01231539.
- [Woj19] Karolina Wojtyniak. “Asymptotyka losowych trajektorii jeu de taquin”. Bachelor’s Thesis. 2019.

INTERDISCIPLINARY DOCTORAL SCHOOL “ACADEMIA COPERNICANA”, FACULTY
OF MATHEMATICS AND COMPUTER SCIENCE, NICOLAUS COPERNICUS UNIVERSITY
IN TORUŃ, UL. FRYDERYKA CHOPINA 12/18, 87-100 TORUŃ, POLAND

Email address: marciniak@mat.umk.pl

INSTITUTE OF MATHEMATICS, POLISH ACADEMY OF SCIENCES, UL. ŚNIADECKICH 8,
00-656 WARSZAWA, POLAND

Email address: psniady@impan.pl